Journal of Medical Robotics Research, Vol. 0, No. 0 (2013) 1–??
© World Scientific Publishing Company

Cognitive AutonomouS CAtheters operating in Dynamic Environments

E. Vander Poorten[a], P. Tran[a], A. Devreker[a], C. Gruijthuijsen[a], S. Portoles-Diez[a], G. Smoljkic[a], V. Strbac[a], N. Famaey[a], D. Reynaerts[a], J. Vander Sloten[a], A. Tibebu[b], B. Yu[b], C. Rauch[b], F. Bernard[b], Y. Kassahun[b], J. H. Metzen[b], S. Giannarou[c], L. Zhao[c], S. Lee[c], G. Yang[c], E. Mazomenos[d], P. Chang[d], D. Stoyanov[d], M. Kvasnytsia[e], J. Van Deun[e], E. Verhoelst[e], M. Sette[f], A. Di Iasio[f], G. Leo[g], F. Hertner[h], D. Scherly[h], L. Chelini[h], N. Häni, D. Seatovic[h], B. Rosa[i] H. De Praetere[j], P. Herijgers[j]

[a] *Dept. of Mechanical Engineering, KU Leuven, Celestijnenlaan 300B, 3001 Heverlee, Belgium*
E-mail: firstáuthor@kuleuven.be

[b] *Faculty Mathematics and Computer Science, Univ. Bremen, Robert-Hooke-Str.5, D-28359 Bremen, Germany*

[c] *Hamlyn Centre for Robotic Surgery, Imperial College London, Exhibition Road, London, SW7 2AZ, UK*

[d] *CMIC, University College London, Hampstead Road, London, NW1 3EE, UK*

[e] *Materialise NV, Technologielaan 15, 3001 Leuven, Belgium*

[f] *Medyria AG, Technoparkstrasse 2, 8406 Winterthur, Switzerland*

[g] *St.Jude Medical Geneva, Chemin du Grand-Puits 42, 1217 Meyrin, Geneva, Switzerland*

[h] *Zürcher Hochschule für Angewandte Wissenschaften, Technikumstrasse 5, CH-8401 Winterthur, Switzerland*

[i] *Department of Cardiovascular Surgery, Boston Children's Hospital, Harvard Medical School, Boston, MA, 02115, USA*

[j] *Department of Experimental Cardiac Surgery, University Hospital Leuven, 3000 Leuven, Belgium*

Advances in miniaturized surgical instrumentation are key to less demanding and safer medical interventions. In cardiovascular procedures interventionalists turn towards catheter-based interventions, treating patients considered unfit for more invasive approaches. A positive outcome is not guaranteed. The risk for calcium dislodgement, tissue damage or even vessel rupture cannot be eliminated when instruments are maneuvered through fragile and diseased vessels. This paper reports on the progress made in terms of catheter design, vessel reconstruction, catheter shape modeling, surgical skill analysis, decision-making and control. These efforts are geared towards the development of the necessary technology to *autonomously* steer catheters through the vasculature, a target of the EU-funded project CASCADE (Cognitive AutonomouS CAtheters operating in Dynamic Environments). Whereas autonomous placement of an aortic valve implant forms the ultimate and concrete goal, the technology of individual building blocks to reach such ambitious goal is expected to be much sooner impacting and assisting interventionalists in their daily clinical practice.

Keywords: Robotic catheters, cognitive surgical robotics, fluidic actuation, automatic registration, 3D reconstruction, SCEM, real-time FEM, continuum robot control, teleoperation, skill analysis, machine learning, autonomous catheter control

1. Introduction

Cardiovascular diseases (CVD) form the single most common cause of death in Europe. With over 4 million deaths per year, CVD is responsible for close to half of all deaths in Europe.[1] In the United States of America (USA) 31.3% of mortalities can be attributed to CVD.[2] Catheter procedures are among the most common surgical interventions used to treat CVD. Due to their minimal access trauma, these procedures extend the range of patients able to receive interventional CVD treatment to age groups dominated by co-morbidity and unacceptable risks for open surgery.[3–6] The downside associated with minimising access incisions lies at the increased complexity and difficult manipulation of the instruments and anatomical targets. These aspects can be attributed to the loss of direct access to the anatomy and poor visualisation of the surgical site. Steering compliant catheters through a fragile cardiovascular system, under the presence of slack, friction and disturbances such as induced by physiological motion, is a complex and demanding task.

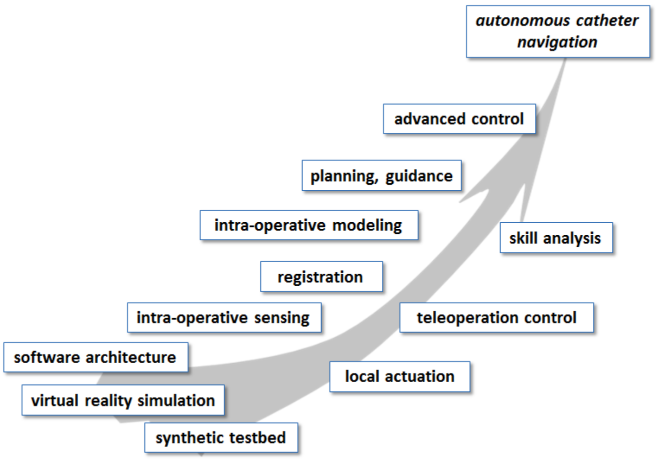

Figure 1. Building blocks on the way towards cognitive autonomous catheter navigation.

The physical and mental load associated with these procedures could lead to human errors[7] and sub-optimal outcome.[8–10] Robotic system developers such as Hansen Medical Inc. (Mountain View, California), Stereotaxis Inc. (St. Louis, Missouri), Corindus Vascular Robotics, Inc. (Waltham, Massachusetts), Catheter Robotics Inc. (Mount Olive, New Jersey) and Magnetecs Inc. (Inglewood, California) responded by offering the clinicians ergonomic workstations from where robotic catheters are steered via teleoperation. While these systems reduce the physical load, improvements are still possible to reduce the mental load, the surgical outcome and the overall level of invasiveness of these procedures.

The EU-funded project CASCADE is set to develop technology to control robotic catheters in a fully *autonomous* manner through the vessel system. It is clear that a great number of technical, clinical and regulatory aspects need to be addressed in order to be able to steer catheters in a reliable manner. Fig. 1 displays a non-exhaustive list of technical aspects that have been identified and elaborated upon within CASCADE. Autonomous catheter navigation requires sophisticated control algorithms (*advanced control*) that steer the catheter according to adequate and timely navigation plans (*planning, guidance*). The adequacy of the generated plans is to be continuously re-evaluated and adjusted as the intervention progresses. The system's response should be in line with that of today's expert interventionalists. Objective assessment of surgical skill is thus a must (*skill analysis*). Plans should reflect the changing reality, which thus needs to be quantified (*intra-operative modeling*). For this, pre-operative data and models are to be put in the right context (*registration*) and then updated through online measurements (*intra-operative sensing/modeling*). While this process takes place implicitly when experts, relying on prior experience, conduct an intervention, it must be formulated more explicitly when autonomous robotic catheters are concerned. Progress in actuation technology (*local actuation*) might be key to further reduce the invasiveness of catheter-based interventions. Damage might be reduced if catheters were more compliant and capable to respond in a coordinated and dynamic manner to accommodate to the fragile environment. Obviously, a flexible and versatile development environment is necessary to prototype all involved technology. Such environment should not be restricted to the *software architecture* which is to be user-friendly and readily expandable, it should also foresee tools for verification and validation, be it computational (e.g. *virtual reality simulation*) or physical (*synthetic testbeds*) allowing quick *in-vitro* testing. A further means to speed up prototyping exists in establishing a *teleoperation control* interface. By giving the surgeons access to the newly developed catheters it becomes possible to benefit from their experience early in the process and derive appropriate steering and guidance methods.

While each building block contributes to the higher goal of *autonomous catheter navigation*, it is believed that progress on individual building blocks could independently create added value on a shorter term. As such the developments could contribute to improve the quality of robot-assisted, but also of manually-executed, catheter interventions. Similarly, although CASCADE focuses on one particular procedure namely TransAortic Valve Implantation (TAVI), the followed approach and key technologies could transfer to other interventions as well, such as endovascular aortic aneurysm repair,[11] transcatheter mitral valve repair or replacement[12] or treatment of cardiac arrhythmia.[13]

The paper is structured as follows. After detailing the clinical application and making the case for robot-assisted treatment in TAVI (Sec. 2), an overview of the progress per building block is offered in Sec. 3-7. Conclusions and directions for further work are sketched in Sec. 8.

2. Case for Robot-Assisted TAVI

2.1. *Clinical aspects of TAVI*

Aortic stenosis is the most common condition requiring valve surgery in the developed world. The incidence of aortic stenosis is increasing due to an aging population. Only in the USA, about 85000 aortic valve replacements are performed annually.[14] When the aortic valve is partially stenosed the strain on the heart muscle increases and the heart function eventually decompensates. Survival rates after onset of symptoms in severe aortic stenosis are dismal, as low as 50% at 2 years and 20% at 5 years.[15] Surgical aortic valve replacement (AVR) is the current standard of care, but it has been estimated that between 30% and 60% of patients do not undergo AVR, owing to advanced age, left ventricular dysfunction, or the presence of multiple co-existing conditions.[16,17] However, with surgical treatment, the prognosis is excellent if the patient is otherwise in relatively good condition.

Patients with high peri-operative risks that were previously classified as inoperable, can now be operated with TAVI.[3–6] When the transfemoral approach is followed, as depicted in Fig. 2, a guidewire, sheaths and catheters are introduced into the femoral artery and navigated through the vessel system. The main function of the guidewire is to find and establish a passage through the remaining opening of the native calcified valve. Typically several attempts are made to cross the opening. The interventionalist will try to limit the interaction force during these attempts so as to minimize the risk for calcium dislodgement. After the guidewire is put into place a catheter with embedded balloon is advanced by sliding it over the guidewire. When centered at the level of the native valve, the balloon is dilated to create space. A delivery catheter with valve implant is advanced next. The interventionalist manipulates the catheter to align the implant perpendicular to and centered with a plane through the aortic annulus. During valve delivery, positioning is based on fluoroscopy. Direct visualisation of the native valve is difficult. Due to the nature of the disease, most stenotic valves are calcified, so the interventionalist will try to infer the position of valve and annulus from observing the calcium. Additionally, angiography dye may be injected to clarify the valve position. Depending on the manufacturer of the implant the valve is self- or balloon-expanded. Care is taken to keep the implant well-aligned during expansion. During the implantation the heart is typically arrested by rapid pacing.

Transfemoral TAVI is less invasive than an open procedure and complementary to a transapical approach, but nevertheless presents considerable challenges and risks:

- operation under low-quality two-dimensional view with limited soft-tissue discrimination;
- patient and surgeon are exposed to ionizing radiation;[18] the contrast agent is demanding for kidneys and could cause allergic reactions;[18]
- bad controllability of catheter; limited bandwidth due to slack, friction, and catheter compliance;
- little control over interaction, possibly causing dislodgement of plaque or calcium, tissue damage or rupture;[19,20]
- lengthy procedure involving many preparatory steps including the introduction of a guidewire, of a catheter to dilate the native valve, of a stabilizing sheet and so on;
- safety issues arise as the surgeon is working in a non-ergonomic manner under high mental and physical load.

Interventionalists experience problems in locating and crossing the opening into the native calcified valve.

- While attempting to cross the native valve undesirable and intense contacts could arise, resulting in dislodgement of plaque or calcium that, taken up in the blood circulation, could end up in the brain and result in stroke;[10]
- to simplify crossing of the valve rapid pacing is applied to arrest the heart temporarily, which should be cautiously used and kept short ($\leq 15s$ according to Webb *et al.*[21]);
- care must be taken that the implant is well aligned and does not migrate inside the heart or towards the coronaries. If not the risk for damaging the heart muscle or blocking the coronaries grows. Morena *et al.* reported an overall mortality during the procedure of 2.3%;[8]

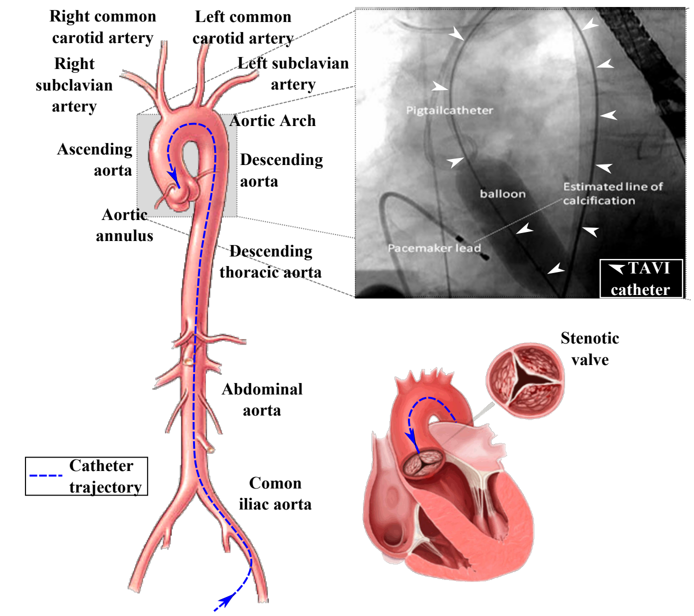

Figure 2. Transcatheter Aortic Valve Implantation; [left] aortic anatomy, trajectory followed by valve placement catheter; [right-up] fluoroscopic image of aortic annulus, balloon dilation to make place for valve implant; [bottom-right] view upon stenotic aortic valve.

- if the cathether and associated valve is badly oriented this may lead to paravalvular leakage.[9]

Compared to surgical aortic valve replacement (AVR), transcatheter aortic valve replacement (TAVR) shows a lower mortality rate (33.9% vs. 35%), yet the prevalence of strokes or major vascular complications is higher in TAVR compared to AVR: 11.2% to 6.5% and 11.6% versus 3.8%, respectively.[2] These figures clearly demonstrate the necessity to further reduce the invasiveness of the procedure.

2.2. *Objectives for robot-assisted TAVI*

While some of abovementioned issues are addressed by state-of-the-art robotic technology;[22,23] existing commercial solutions from Hansen Medical, Corindus, Stereotaxis Catheter Robotics or Magnetecs are not intended for TAVI.[22] It is unclear whether they meet the requirements in terms of compliance, payload, bandwidth and precision needed to align valve implants. Whereas the catheters steered by the NIOBE (Stereotaxis) and CGCI (Magnetecs) systems are compliant, they are not designed for the payload of TAVI. Systems from Hansen Medical or Corindus rely on exchange of several assemblies of catheters, guidewires and guiding sheaths. Operating those fairly stiff devices in a fragile, calcified environment is not without risk for calcium dislodgement or tissue damage.

The high number and exchange of instruments is considered disadvantageous as air bubbles, responsible for air embolisms, could be introduced as well.[24]

From discussions with clinicians the following needs were established. A solution is needed (a) dedicated to TAVI, (b) that is less dependent on damaging imaging techniques; (c) cuts down in the number of components (guidewires, sheaths, catheters), which could therefore reduce execution time; (d) limits the need to arrest the heart through rapid-pacing; (e) offers improved awareness of and control over the interaction between catheter and vasculature, e.g. identifies side-branches and risk prone areas such as plaques, calcification or aneurysms; (f) allows more detailed control of the catheter tip (aiming at improved valve positioning and alignment); (g) reduces physical and mental workload; (h) when operating autonomously, provides a predictive display indicating future catheter actions; (i) is interruptable, allowing smooth transfer to teleoperated or manual intervention. Some quantitative requirements are listed in Table 1. Note that these values are indicative and must be confirmed experimentally e.g. be through the technology developed in CASCADE developed technology.

To address these needs, in accordance with the basic vision expressed in Fig. 1, CASCADE aims to progress following key technologies: (a) catheter actuation (SubSec. 4.2); (b) intra-operative sensing (SubSec. 4.1); (c) intra-operative modeling (Sec. 5); (d) skill analysis and planning (Sec. 6); (e) advanced robotic control (Sec. 7), towards a new type of *cognitive* catheter that *autonomously* navigates through the vessels and, in the envisioned use case, is capable of adequately positioning and aligning valve implants. A dedicated software framework, a carefully engineered Virtual Reality (VR) environment and synthetic test-beds, described next (SubSec. 3.1-3.3), are considered, key enablers, providing essential support in prototyping and deploying all developed hardware and algorithms.

Table 1. Selected requirements for robotic TAVI established after discussion with clinicians; (1) most distal part from valve implant to tip should be limited in length not damage the heart muscle; (2) mainly to push through trocar; (3) obtained from.[25]

catheter O.D.	$\leq$ 7mm
minimal effective length	$\geq$ 1150mm
maximal lenght distal to valve	$\leq$ 50mm (1)
minimal bending radius	30mm
insertion - retraction force	40N (2)
distal DoFs, number	2 or more
–, velocity	$\approx$ 210mm/s (3)
–, acceleration	$\approx$ 3900mm/s^2 (3)
–, bandwidth	5Hz
tip position accuracy	1.3mm
shape measurement accuracy	3 mm
tip interaction force	$\leq$ 5N
total execution time	$\leq$ 10min

3. Instruments for prototyping catheter-based interventions

3.1. *CASCADE software framework*

Fig. 3 gives a glance on the interface of the software architecture that has been devised.[26] The architecture addresses the needs from software developers, who want a platform that allows efficient development and prototyping, and interventionalists for whom this forms the main window to the vasculature, the catheter and a vast amount of information that is generated by sensors and models. To ensure reliable control and timely operation the framework follows a component-based philosophy. All functionality is encapsulated in loosely coupled components. The Robot Operating System (ROS [27]) messaging system is used to communicate between components. Components that require hard real-time operation rely on Open Robot Control Software (OROCOS [28]). Components can be switched on and off on the fly allowing quick configuration of the system for any particular test. Data can be logged and replayed for analysis. Through a hardware abstraction layer abstraction is made of the actual hardware that is used. In fact, software components are ignorant as to whether they are communicating with a real catheter and testbed or with a virtual catheter. Neither does the catheter driver know whether the commands it is receiving come from any of the autonomous controllers or from an operator who tele-operates the catheter through a joystick. The adopted architecture promotes embedding redundancy at multiple levels, which is advantageous from safety perspective. Not only can sensors and algorithms be fused relatively easy, when components underperform or sensors brake, other sensors or even virtual sensors can come in. The user can overtake the procedure to *teach* difficult parts or as a fall-back if all other fails.

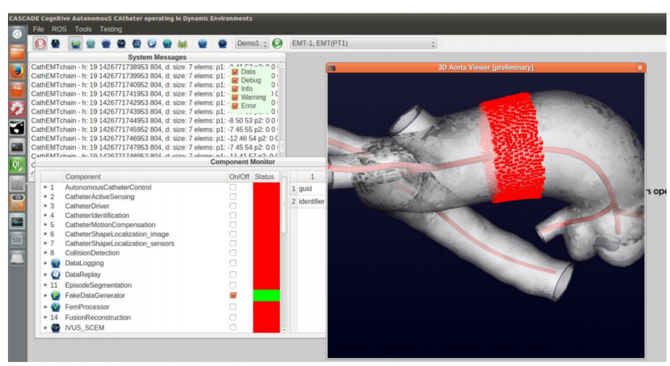

Figure 3. View upon CASCADE development environment: [left] functionality can be selected online; [right] Aorta3DViewer, one of the visualisers available during the intervention; highlighted parts of three-dimensional (3D) mesh undergo finite element analysis.

3.2. *Virtual Reality Environment*

While the catheter is inserted into the vasculature, it flexes, bends and adapts its shape to the surrounding vessel. The overall interaction with the vessel is highly complex and cannot be captured by a simple set of analytical formulas. A VR environment has been built to simulate this behaviour and speed up development and testing. Compared to real-world experiments, simulations in VR requires practically no setup time; experiments can be repeated at wish. Another important feature is the availability of ground-truth information which simplifies assessment of the performance of algorithms. Clearly, the realism of the simulation environment is crucial as it determines the confidence one can attach to conducted analyses.

Methods based on mass-spring models,[29,30] finite elements[31] or discrete versions of the Elastic Kirchhoff Rod theory[32,33] have been proposed to simulate guidewire or catheter behaviour. CASCADE progresses the work by Konings *et al.* who predict the behaviour of a guidewire by minimizing the joint energy of guidewire and surrounding vessel.[34–38] The underlying idea is that since the overall motions are relatively slow, a quasi-static approximation of the catheter/vessel is justifiable. Under this assumption the catheter comes at rest in an equilibrium state after each simulation step taking on a shape where the aggregated energy (of catheter and vessel) is minimal. The algorithm of Konings *et al.* , originally designed for simulating guidewires, was expanded for simulating robotic catheters, relying on more realistic friction models and allowing simulation of distal actuated sections.

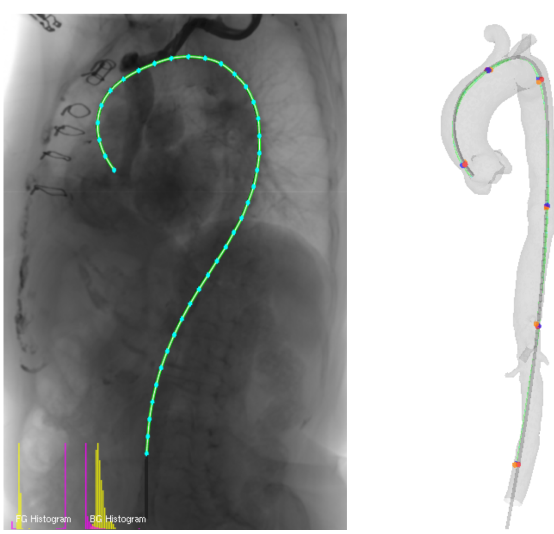

Figure 4. CASCADE VR simulation environment for rapid prototyping of catheters and algorithms. Here, sensor-based reconstruction of the catheter's shape (green line) is evaluated by comparison with the simulated ground-truth (black/grey line); [left] fluoroscopy viewer - [right] catheter 3D viewer.

VR was used a.o. for prototyping novel catheters (SubSec. 4.2 and 4.1), generating data-sets for machine-learning (SubSec. 7.3), testing modeling techniques (SubSec. 5.2), but also for user tests (SubSec. 6.1, 6.3) and catheter control experiments (SubSec 7.2) were it helps synthesize controllers for experiments in the synthetic testbed.[39–41] Fig. 4 gives a view upon the VR environment featuring apart from a 3D-viewer a.o. a fluoroscopy viewer providing familiar images to the clinicians.

3.3. *Synthetic perfused test-bed development*

A higher level of evidence or confidence is associated with real-world experiments. Both from an ethical viewpoint[42] as for practical reasons it is found opportune, to invest in the development of dedicated synthetic testbeds to validate algorithms and hardware. Requirements for such testbeds, further detailed by Kvasnytsia *et al.*,[43] are:

- geometry containing ascending aorta with left and right coronary artery bifurcation, aortic arch with brachiocephalic, left common carotid and left subclavian artery, abdominal aorta with mesenteric, left and right renal and common iliac artery;
- geometric accuracy and reproducability - consistent to the 3D data used a.o. in the virtual reality and other computational models;
- realistic mechanical properties - responding naturally to physiological phenomena and catheter interaction;
- compatibility to relevant sensors a.o. with Magnetic Resonance (MR), Computed Tomography (CT), electromagnetic tracking (EMT) and ultrasound (US);
- versatility - replicating patient specific anatomy e.g. aneurysms, calcifications or other risk prone areas;
- robustness - allowing frequent passage of experimental catheters;
- cost efficiency - enabling validation under varying conditions and geometries;
- good transparency, allowing visual confirmation of the catheter and the use of cameras to simulate fluoroscopy.

Since customization of current commercial bench top models such as the silicon models provided by Elastrat Sarl (Genéve, Switzerland), United Biologics (Tustin, California) or Fain Biomedical Inc. (Nagoya, Japan) is costly and only offers limited control over material properties, it was decided to design and develop dedicated test-beds and models for CASCADE. Several testbeds were engineered as summarized in Table 2. All testbeds were built from real patient data. CT data was segmented using the Mimics Innovation Suite® (Materialise NV, Leuven, Belgium). This data was also used in the VR environment (SubSec. 3.2) allowing comparison and transfer of learned knowledge.

First, some simple 2D testbeds were built whereby a segmented aorta was projected onto a 2D plane. The vessel lumen was laser cut from a polycarbonate plate which was put in a sandwich structure with two other polycarbonate plates. Along similar lines a 2D deformable model

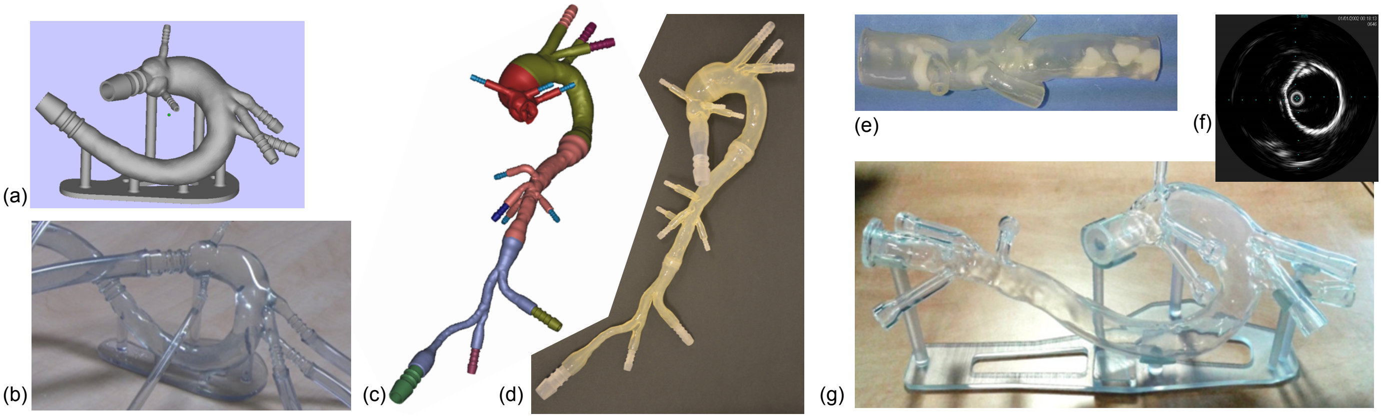

Figure 5. 3D printed testbeds - (a)/(b) CAD and printed rigid SLA model; (c)/(d) CAD and printed HeartPrint™Flex model; (e)/(f) multimaterial inkjet 3D model from HeartPrint™and IntraVascular UltraSound (IVUS) image. Calcifications visible in (e) appear clear in corresponding IVUS image (f); (g) New hybrid silicon casted model showing good transparency and flexibility.

was made. Silicon (EcoFlex 0050, FormX, Amsterdam, The Netherlands) was poured in a polycarbonate mold to form a 7mm thick aortic wall, this was then sandwiched between 2 polycarbonate plates.

Rigid 3D models were made from stereolithography (SLA, wall thickness 2 mm, surface smoothing and cosmetic finishing step, Fig. 5.a,b). It was verified that 95% of the surface elements lie within an interval of $[-0.5, 0.5]$ mm from the original model. So it was found justifiable to use the Computer-Aided Design (CAD) data as a ground truth for the model's geometry.

For the more advanced experiments deformable 3D models were used. A first set was printed from HeartPrint™Flex (wall thickness 1.5 mm). The mechanical properties approach those of the human vasculature[44] as was verified through uniaxial tensile tests. Utilizing multimaterial inkjet, 3D printing calcifications can be incorporated into this model (Fig. 5.e). Additionally, the model showed excellent US compatibility. Fig. 5.f shows also the calcification. The robustness of this material was found restrictive for CASCADE as unlimited passage of catheters is required. Therefore a modular setup was made (Fig. 5.c/d) to easily replace damaged parts. In parallel, a novel hybrid silicon casting technique was developed. These models showed superior robustness and excellent transparency (Fig. 5.g), good ultrasound compatibility and mechanical properties. Embedding calcifications in the hybrid silicon cast process is costly as it would call for many manual steps and was therefore not attempted at this point.

A dedicated perfusion system was made to replicate the blood circulation. The system consisted of a volumetric pump that injects a controlled volume of fluid into a chamber connected via two non-return valves (simulating the mitral and aortic valve) to the synthetic vasculature. Calcium and mineral oil was added to the perfused water so as not to jeopardize the visibility while offering similar ultrasound properties and friction as in the vasculature.

A support structure was designed to provide anatomically correct positioning of the vessel. The support was designed to allow, upon perfusion, deformation that is similar to the physiological motion from heartbeat and breathing.

Table 2. Properties of the in CASCADE developed synthethic test-beds, legend: [×] pass; [o] borderline; [ ] not investigated

		full aorta	deformable	robust	transparency	US compatible	calcification
2D polycarbonate				×	×		
2D Ecoflex 0050		×		×	×		
SLA	Fig. 5.a/b			×	×	×	
HeartPrint^{TM}	Fig. 5.c/d/e/f	×	×	o	o	×	×
HybridSiliconCast	Fig. 5.g	×	×	×	×	×	

4. Self-aware dynamic catheters

Excellent dynamic properties are needed to precisely align a valve implant while the heart is still beating. Good knowledge of the own pose - catheter shape - with respect to the surrounding vasculature is essential to determine appropriate steering actions. This section describes the progress in catheter development towards catheters that are *self-aware* (SubSec. 4.1) and that can safely operate in a dynamic and deformable environment (SubSec. 4.2).

4.1. *Intra-operative sensing*

As the vasculature is compliant and subject to deformation from physiological phenomena, but also distorts through the inserted guidewires and catheters, one should not rely too much on pre-operative data for navigation. In clinical practice interventionalists use fluoroscopy and inject contrast agent to get a better sight on the vasculature. In order to reduce the dependency on and complement the information obtained from fluoroscopy, intra-operative *proprio-* and *exteroceptive* sensors can be used providing up-to-date measurements from within the vasculature.

4.1.1. *Sensors for catheter proprioception*

While fiber optic sensing technologies are seen as a promising method for catheter shape sensing,[45,46] this technology is still under development and was only briefly touched within CASCADE (Fig. 6(e)).[47] Electromagnetic tracking was found a convenient and mature alternative for catheter proprioception.[11] A number of miniature EMT sensors (Aurora, Northern Digital Inc. (NDI), Waterloo, Ontario, Canada) can hereto be distributed over the catheter length. In CASCADE for example an Aurora Micro 6 DoF EMT sensor with 0.8mm outer diameter (O.D., Fig. 6(a)) is integrated at the catheter tip and 0.5mm O.D. 5 DoF Aurora sensors are distributed strategically along the catheter length. The EMT sensors measure the catheter pose at 40Hz, with a precision of about 0.9 mm and 1 deg within the field generator's working volume. An adequate distribution of EMT sensors was determined in VR. By avoiding sources of external disturbance and using an NDI Tabletop field generator distortions have been kept minimal. Compensation methods[48] might become necessary when moving towards the clinic.

4.1.2. *Sensors for exteroception*

Information on the relative distance to the vessel wall, on the proximity of aneurysms, bifurcations, plaque or calcium, is extremely valuable as such knowledge could be used to steer the catheter more intelligently past these risky areas. Where now clinicians are to infer this information indirectly e.g. from fluoroscopy and contrast agent, through catheter-mounted exteroceptive sensing it becomes possible measure and hence exploit this information in a more direct fashion. Amongst the different imaging modalities such as based on ultrasound (intravascular ultrasound or IVUS),[49] optical coherence tomography (OCT),[49] angioscopy,[50] MRI[51] or infrared vision,[52] IVUS is found a mature and widely used technique. Aside from its capability to detect vascular abnormalities, withing CASCADE it is used to capture the entire vessel wall (i.e. also the more normal parts). For example the Visions PV.035 ® or predecessor PV8.2 ® (Volcano Corporation, San Diego, California) provides a 30mm radius cross-sectional view of the vessel at 20Hz update rate, and this along a section perpendicular to the probe. Forward Looking IVUS probes (FLIVUS) would find great use e.g. to detect the aperture in the native calcified valve, but this technology is still under development.[53] Flow sensing could be used to provide similar information as a peak in blood flow is expected in the vicinity of the valve opening. In a sense flow gives us thus also a kind of forward-looking (of side-ways at side-branches) view into the vasculature. Fig. 6(d) shows a flow-sensing catheter (TrackCath, Medyria AG) that has been used. Also force sensing could help improve safety as it would allow avoiding large forces/and stresses from developing at the catheter tip. The TactiCath™, a 3.5mm diameter, 1g force resolution, fiber optic tri-axial Fabry-Perot force sensing catheter (Fig. 6(b) and (e)) (St. Jude Medical, St. Paul, Minnesota) was tested within CASCADE.

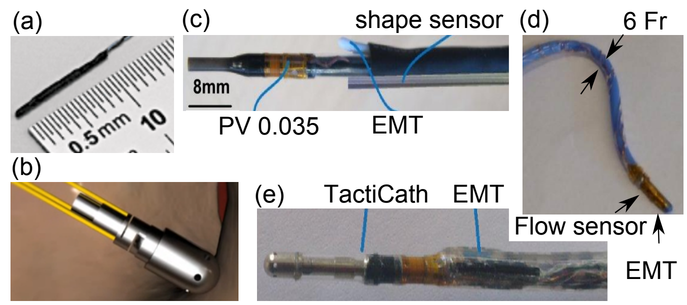

Figure 6. Selection of sensors and catheters with embedded sensors: (a) 6DoF EMT sensor (Aurora® NDI); (b) sketch of TactiCath™force sensor; (c) catheter with IVUS and EMT; (d) flow-sensing catheter with embedded EMT; (e) force-sensing catheter with EMT.

4.2. *Fluidic actuation*

Traditional cable-actuated catheters suffer from friction and non-isotropic behaviour. These effects complicate dynamic coordinated control of the distal Degrees of Freedom (DoFs) and make it difficult to maneuver the catheter precisely in fragile and dynamic environments such as in the vicinity of the aortic annulus.[54] Several researchers have looked into catheter control in a dynamic context. Kesner *et al.* introduced an approach for mitral valve repair featuring motion-compensation to account for heart beat.[55,56] While appealing, the system only deals with a single DoF, thus not allowing adjustment of the orientation. Vrooijink *et. al.* proposed a robotic delivery sheath for transapical TAVI.[57] Similar to traditional commercial robotic catheters, its tip is articulated by two pairs of antagonistic tension wires. Friction and backlash within the system limit the dynamic range. This limitation will be even more problematic when moving to transfemoral TAVI. Shape Memory Alloy (SMA)-based solutions[58,59] also exhibit a fairly slow dynamic response due to the thermomechanical phenomena involved. SMA actuation compares favourably to cable-based approaches when many active DoFs are needed. As the number of cables rises these catheters become increasingly stiff, making it easier to damage surrounding tissue. For a fairly recent survey of robotic catheters refer to Fu *et al.*[60] Fluidic actuation, as progressed by Ikuta *et al.*, was found to be among the more appealing approaches as the associated compliance offers a certain amount of intrinsic safety.[61] At the same time increasing the number of DoFs does not necessarily imply a prohibitively stiff catheter. Whereas, Ikuta made use of a series of bellows supplied by a single pressure line, the authors looked at more powerful actuation methods, embedding McKibben muscles in their catheters.[62] The VR environment (SubSec. 3.2) was used to determine appropriate location, length and bending characteristics of the muscles for a TAVI[39] catheter.

Fig. 7 shows the distal part of a catheter with two 2DoF bending segments and 4 pairs antagonistic muscles. The muscles were made with balloons from 1.96mm O.D. Silastic RX50 medical grade tubing (Dow Corning Corp., Michigan, USA) and a 2.2mm O.D. metallic braid (29° braid angle). A 7mm diameter laser cut nitinol backbone structure completes the active element. This catheter shows excellent robustness, controllability and a bandwidth exceeding 8Hz.[63] However, since the muscles are fairly large there is no space for a working channel. Efforts were conducted to miniaturize the muscles. By shifting to a polyimide braid and 0.94mm O.D. tubing muscles of 1.1mm O.D. were obtained, opening up good perspectives for further miniaturisation.[62,64] These new muscles were incorporated in the final valve deployment catheter.

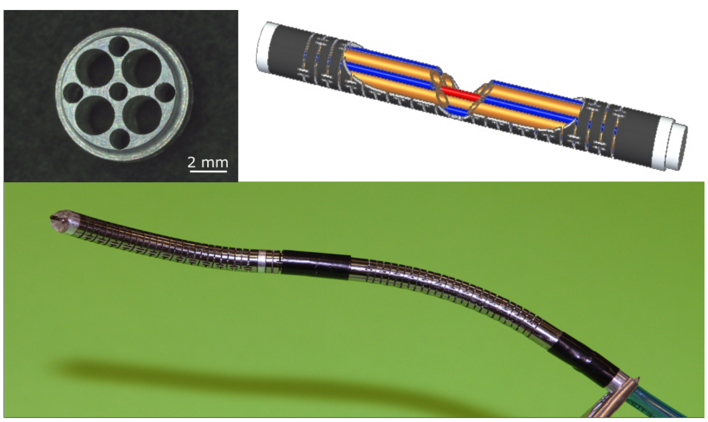

Figure 7. Picture and CAD-drawing of a distal section of a fluidic actuated catheter[62–64] with 4 pairs of antagonistic muscles inside a nitinol backbone.

4.3. *Valve deployment catheter*

After experimentation with the different actuation and sensing technologies, the valve deployment catheter as depicted in Fig. 8 was designed. The catheter contains two active segments, one at each side of the valve implant. In addition to eight supply lines (4 × 2 muscles) a ninth central supply line serves to inflate a balloon that is to expand the valve implant. For convenience the Edwards Sapien valve (Edwards Lifesciences, Irvine, California, USA) is shown in a semi-inflated position. When crimped, its O.D. - and that of the entire catheter - will be not more than 7mm. As

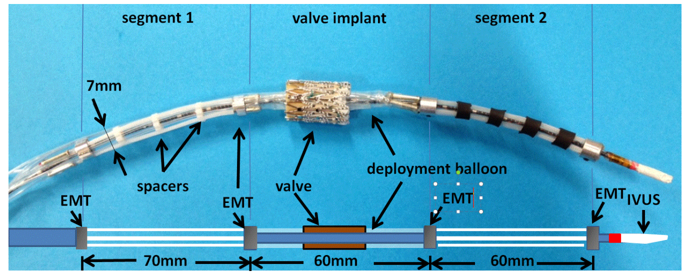

Figure 8. View upon valve deployment catheter consisting out of an active segment proximal to and an active segment distal to the valve that is going to be deployed. 6 EMT sensors are distributed over the catheter length, further incorporated are an IVUS sensor and flow sensor mounted at the catheter tip.

the developed controllers are geared to avoid contact between the catheter tip and the vessel wall alltogether, flow sensing is selected in favour of force sensing in this version. The catheter is further equiped with 6 EMT sensors (4 indicated) and an IVUS sensor at the tip. The current version meets the requirements in terms of total O.D., effective length and achievable bending radius. However the length of the segment distal to the valve should be still reduced in order to avoid contact with the heart muscles. Also extra effort is to be paid to improve the robustness of the catheter as some muscles broke after a limited number of passages through the vasculature.

5. Intra-operative modeling

Self-aware catheters acquire timely information from within the vessel. Information that, after some processing and modelling, could offer additional insights and enhance the operator's or controller's awareness of the state of the catheter/vessel system. A number of different intra-operative modeling techniques, described next, demonstrate how intra-operative (intravascular) measurements could be exploited advantageously.

5.1. *Automatic registration of pre-op data*

A first obvious expansion of current practice consists of making better use of the pre-operatively acquired MR/CT data by augmenting the two-dimensional fluoroscopy images with it. For this to work both datasets need to be aligned or *registered* properly. A review of the basic registration schemes is provided by Sra *et al.*[65] Current registration methods, including those applied on catheter procedures,[66–68] require a significant amount of human interaction. As this is both time-consuming and error-prone these methods are hardly applied in clinical practice. Fully automatic registration technology would allow a smoother integration into the surgical workflow as user involvement could remain limited to supervision.

Through use of catheters with intra-operative, intravascular sensing capability this becomes possible. For example in earlier work, Zhong *et al.* used IVUS to automatically collect a dense point cloud[69] that is then registered to the pre-operative data using the Iterative Closest Point (ICP) algorithm. While reducing the efforts for registration, user interaction is *not* eliminated with Zhong's appraoch. This is because ICP is sensitive to outliers and requires a suitable initial registration guess to work properly. Within CASCADE a fast, global registration algorithm, relying on catheter embarked sensors has been developed.[70] The algorithm is fully automatic, but could in fact run continuously in the background spawning updates and improvements at regular intervals. The proposed algorithm is a branch-and-bound stochastic algorithm that was adapted from Papazov *et al.*[71] The algorithm consists of an initialisation step where pre-operative MR/CT data is pre-processed and the Euclidean 3D distance transform is computed for the voxelized mesh. The branch-and-bound algorithm is applied next. The sampling method employed by Papazov *et al.* is refined to get a more uniform sampling of the transformation space. Also a new cost function has been proposed. In order to quickly and safely obtain sufficient intra-operative data on the vasculature we propose to not only consider the *surface points*, i.e. the points located on the vessel wall, but also to account for *lumen points*. Lumen points are measurement points of the catheter at locations where it does not contact the vessel wall. The idea is that incorporating knowledge on which space is unoccupied might speed up the convergence, of course under the assumption that the catheter does not depart from the vasculature (e.g. because the vessel ruptures). In the case of a sparse set of surface points, the proposed registration algorithm[70] is able to double the registration accuracy thanks to these lumen points. The algorithm has been validated on a deformable Elastrat phantom model, similar to the HybridSiliconCast described in SubSec. 3.3. The approach was applied on 2 different catheters. A first EMT-IVUS catheter was equipped with an IVUS PV8.2 sensor at its tip. Additionally, it has a single 6DoF EMT sensor at its tip as well as 2 5DoF EMT sensors at respectively 80 and 160mm from the tip.

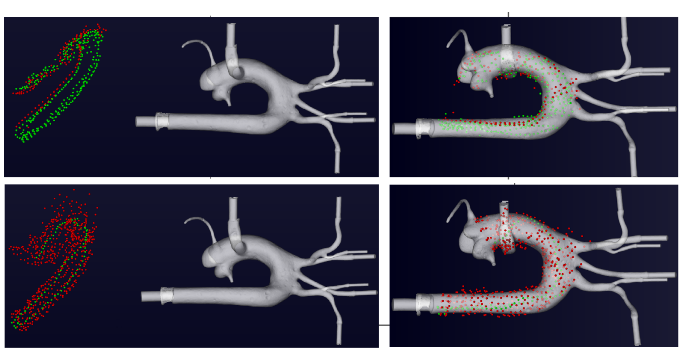

Figure 9. Data-to-model registration result for (upper row) EMT-force catheter, and (lower row) EMT-IVUS catheter. Surface points are depicted in red and lumen points in green.[70]

A second EMT-force catheter possesses a TactiCath force sensor and 6DoF EMT sensor at its tip and carries 5 additional 5DoF EMT sensors spaced at 80mm intervals along the catheter length.

Fig. 9 shows the result of the registration algorithm with both catheters. EMT sensors are used to identify surface points and lumen points, whereas IVUS and force sensing is used to identify surface points only. The total global registration process achieved an average registration error of 3.9 mm after 4.8 s computation for a catheter equipped with force and EMT sensors, and of 5.1 mm in 7.4 s for a catheter with embedded IVUS and EMT sensors. This is comparable to accuracies needed for clinical application, as reported by Dong *et al.*[67] However, the computation time is significantly reduced to only a few seconds, and no time is added due to the registration process itself, since it does not interfere with the clinical workflow.

5.2. *Catheter shape reconstruction*

Knowledge of the entire 3D-shape of the catheter could help planning and assessing risks associated with future steering actions. At present interventionalists rely on conventional monoplane fluoroscopy, where all depth information is lost, for estimation of the catheter shape. Via the EMT sensors embedded along the catheter length, an online 3D estimate of the catheter shape can be obtained. Two such methods have been worked out.

A first method makes use of a set of 5-DoF EMT sensors embedded along the catheter length. These sensors provide pose information at discrete locations along the catheter, which through a nonlinear cubic spline fitting, gives a 3-dimensional estimate of the shape. The objective function used in this fitting tries to minimize the pose error, maintain the known distance between sensors (assuming incompressibility along axial catheter length) and to reduce the overall bending energy of the resulting curve. Fig. 10 shows an example of EMT-based shape reconstruction in the VR environment. Note that when inserted deeper, the estimation error at the proximal part, whereas prediction accuracy at the distal part remains of acceptable quality.

A second approach fuses EMT data with a catheter tracking algorithm based on fluoroscopy. The main rationale is that if fluoroscopy is present anyway, its use can at least be reduced to anatomical risk-prone areas where a highly accurate and reliable reconstruction of the catheter shape is required. Using a B-spline tube model[72] within a probabilistic framework derived from Bibby *et al.*'s work,[73] the 2D dense information extracted from fluoroscopic images is combined with the 3D discrete pose of the EMT sensors. In constrast to fluoroscopy-based sensing, the fused approach offers a full 3-dimensional catheter shape estimate. Compared to pure EMT-based shape sensing, the approach is expected to show greater robustness and accuracy, as the reconstruction algorithm becomes less sensitive to internal and external electromagnetic interferences. It could potentially relieve the need of using dedicated

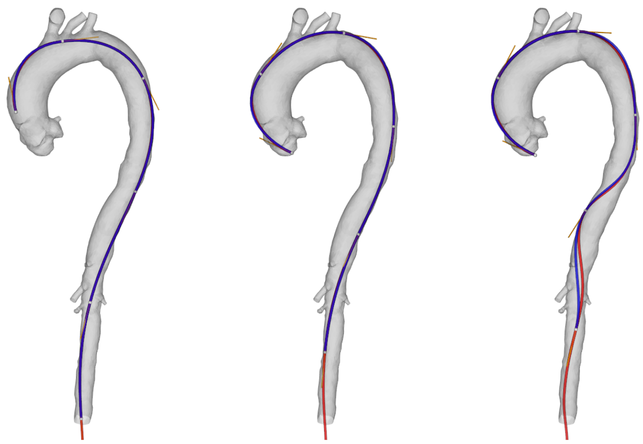

Figure 10. EMT-based shape reconstruction in VR; ground-truth in red; root mean square (RMS) and Hausdorff errors are [left] e_{rms}=0.46mm, e_{h}=1.34mm, [center] e_{rms}=0.61mm, e_{h}=1.41mm, and [right] e_{rms}=1.61mm, e_{h}=4.39mm.

shielding or performing tedious calibration procedures to compensate for electromagnetic field distortion[74,75] which do not integrate well with the current surgical workflow. Promising results for latter approach were obtained from the VR experiments (Fig. 4). Table 3 summarizes the RMS and Hausdorff distance between the simulated ground-truth and the reconstructed catheter using respectively the first ($e_{rms,emt}$,$e_{h,emt}$) and second ($e_{rms,fus}$,$e_{h,fus}$) approach. Note that white noise with standard deviation of 1.5mm was added to the virtually generated EMT sensor data in order to simulate electromagnetic disturbances.

Table 3. Evaluation of shape reconstruction errors [mm] using EMT-based and fusion approaches for different catheter insertion lengths L [mm] and number of EMT sensors in VR simulation.

L	# sensors	$e_{rms,emt}$	$e_{rms,fus}$	$e_{h,emt}$	$e_{h,fus}$
175	3	1.17	0.59	1.52	0.88
275	4	2.06	1.68	3.96	3.40
385	5	2.76	2.31	4.46	4.43
485	6	1.56	0.88	3.24	1.79

5.3. *Intra-operative vessel modeling*

Whereas the methods from SubSec. 5.1 and SubSec. 5.2 already reduce the dependency on X-ray fluoroscopy and contrast agent, they do not yet exploit the full potential of intra-operative sensing. Inspired by robotic techniques such as SLAM (Simultaneous Localisation and Mapping) whereby without any prior knowledge a robot moves through its environment and incrementally builds up a 3-dimensional map of its surrounding, CASCADE introduces SCEM: 'Simultaneous Catheter and Environment Mapping'.[47] SCEM is a robust and real-time vessel reconstruction scheme for endovascular navigation based on IVUS and EM tracking. The concept is similar to SLAM, the catheter moves up from the groin, scans the environment - the surrounding vessel - by using IVUS and stitches the obtained 2-dimensional scans to each other to form a 3-dimensional representation of the vessel wall. In principle, an up-to-date reconstruction of the vessel could be done in such manner strongly reducing the need for fluoroscopy.

A number of processing steps, depicted in Fig. 11, are necessary to reliably extract the vessel contour out of the raw IVUS image. Once the contour is obtained, it can be expressed in the absolute coordinate frame of the electromagnetic (EM) field generator through a simple kinematic transformation (an EMT sensor positioned within the lumen of the IVUS sensors provides the absolute pose of the US probe). Scans can then be stitched to form a closed 3D vessel model. For this approach to work the transformation between IVUS and EMT sensor frames must be known. It suffices to conduct such calibration once as this is a catheter-dependent property. A possible calibration manner consists of scanning a known calibration object with the IVUS sensor on the EMT-IVUS catheter and afterwards probing the calibration object with a bare Aurora calibration sensor to get its pose in Aurora coordinates. From matching the scans, the calibration can then be retrieved. Whereas the previous implementation treated observations from IVUS and EMT as exact,[47] the newer SCEM+[76] algorithm takes uncertainty into account. This reduces the

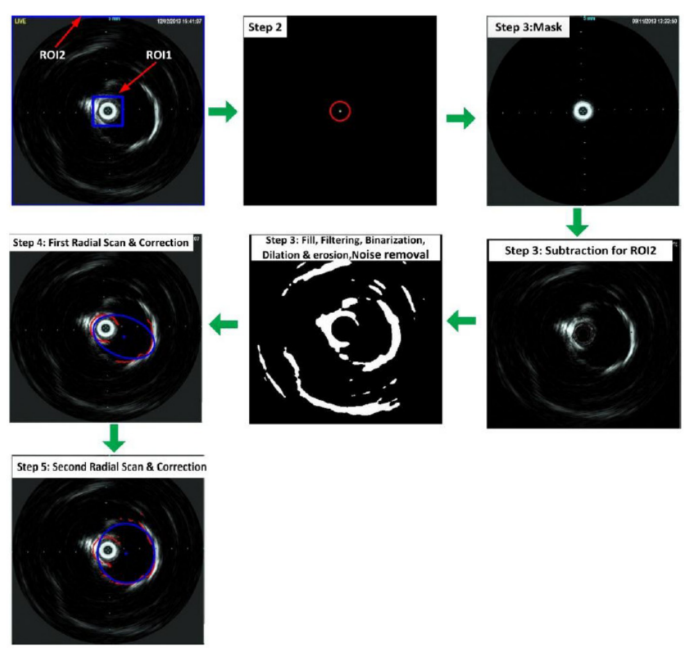

Figure 11. Processing steps to extract the vessel contour from IVUS.[47] The computed countour is stiched to previous scans to form an intra-operative vessel model.

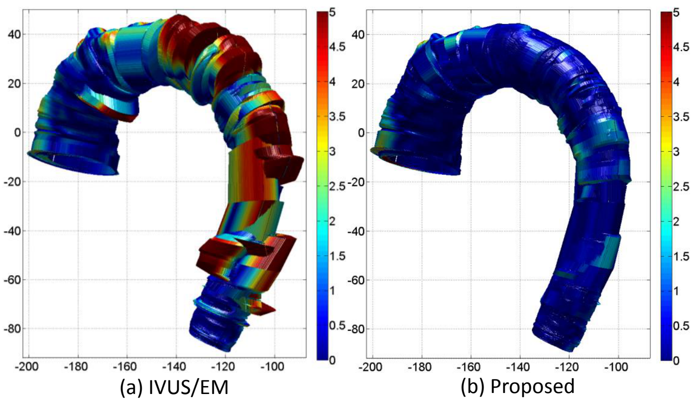

Figure 12. 3D vessel reconstruction with abrupt catheter motion (errors in mm); (a) SCEM and[47] (b) SCEM+ considering uncertainty and pre-operative vessel morphology.[76]

vulnerability to errors in the observations and abrupt catheter motion. SCEM+ first extracts from the IVUS image the contour which represents the inner cross section of the aorta. Then, the vessel reconstruction is formulated as a nonlinear optimisation problem by considering both the IVUS contour and the EM pose as observations, as well as pre-operative vessel morphology. By considering the errors and the measurement uncertainty in the optimisation, SCEM+ is more robust. Especially in the presence of abrupt catheter motion a significant improvement can be noticed. Experiments were conducted on both the printed SLA-model and the HeartPrintFlex testbed. Outcome for the latter is depicted in Fig. 12a and Fig. 12b for SCEM and SCEM+ respectively. The figure clearly shows the much smoother reconstruction from SCEM+. The mean error for SCEM+ on the SLA testbed were about 0.6mm, whereas those on the deformable HeartPrintFlex errors were on average 0.3mm. It is believed that the improved performance for the reconstruction of the HeartPrintFlex aorta is mainly caused by its superior US-properties.

5.4. *Mechanical vessel modeling*

Up-to-date geometric vessel models only capture part of the interaction as they do not provide a measure of the forces that are exerted. If incurred stresses are too high this could lead to dangerous situations: tissue damage, vessel rupture, dislodgement of calcium or atherosclerotic plaque.[19,77] Through Finite Element Modeling (FEM) of both vessel and catheter it would be possible to get an improved understanding of these aspects. Within CASCADE efforts significant steps were made towards intra-operative use of finite element aorta models. With such technology interventionalists could re-plan actions and e.g. retract the catheter when observing stress levels rise unacceptably. Similarly advanced control schemes could exploit this information and give precedence to less stressful trajectories.

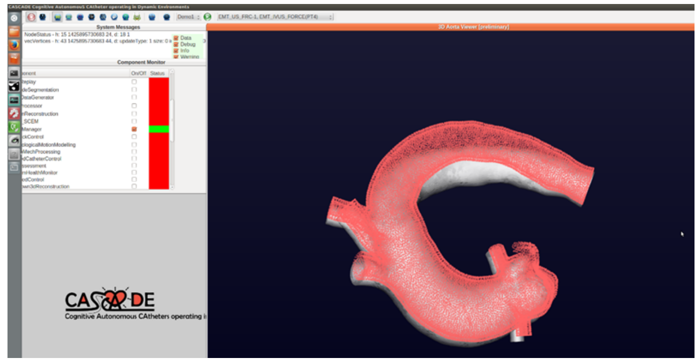

Figure 13. Real-time update of aorta mesh accounting for global deformation; input is here an updated geometric model (aorta center-line) obtained from SCEM. The original aorta mesh is depicted in grey; overlay of mesh in red.

Creating a real-time FEM model of the vasculature is far from trivial. Starting from a general approach by Gregson *et al.*[78] several attempts and modifications were made to generate a high-quality hexahedral mesh of the aorta. While the minimum element quality was improved substantially (scaled Jacobians higher than 0.1), this was found still insufficient for proper use. Further improvements are needed. In the meanwhile a general purpose graphics processing unit (GPGPU) implementation of the Total Lagrangian Explicit Dynamic (TLED) algorithm[79] for soft tissue FEM simulation was made[80] as its good parallelization properties showed good potential for speeding up the computations. Fiber reinforced nonlinear constitutive models[81] necessary for simulating aortic tissue were implemented and tested in the TLED. Significant performance improvements were attained, with for simple test-cases, performance speed ups of 30 to 120 times compared to computation time from current commercial solutions.[80] Methods were futher devised to allow fast online selection of a specific region of interest. The area around the catheter tip is of particular interest as large stresses could develop here. Fig. 3 shows the result of a selection around the tip region. In addition, a global deformation algorithm was developed. Based on an updated aorta centerline (e.g. from SCEM), the entire aorta mesh can be updated (Fig. 13). Then the updated region of interest is selected for computation. By combining these components with fast collision detection schemes it would become possible to get representative estimates of ditributed stresses in the vessel.

5.5. *Detection of risk prone areas*

Risk prone areas such as regions with plaque or calcification deposits are better avoided all together. These can be considered immobile and therefore their pose is primarily determined by the overall deformation of the aorta. Based on estimates of the locations of these areas, e.g. from pre-operative CT (SubSec.5.5.1), relying on registration (Subsec.5.1) or reconstruction techniques (Subsec.5.3), their location can be estimated intra-operatively. Additionally their location can be inferred from direct measurements e.g. from IVUS. This is for example demonstrated for the case of estimating side branches (SubSec.5.5.2).

5.5.1. *Detection of calcification*

Different approaches for detecting calcification in CT images based on supervised machine learning were considered.[82] With the so-called pixel-wise approach, each pixel in the image is treated separately as a sample that is classified based on statistical properties from the local neighbourhood. A classifier such as a support vector machine (SVM) can be used here. In contrast, with a segment-wise approach, the image is over-segmented. Similar pixels are clustered prior to feature extraction. Each segment is then classified as a whole. The simple linear iterative clustering (SLIC) technique[83] has been applied on the latter. SLIC can be tuned by selecting an appropriate amount and an appropriate level of compactness of the segments. In general, over-segmentation reduces the amount of training samples needed to train the classifier. Instead of classifying pixels, whole segments are treated as input for the classifier. The distribution of intensity values in the segment is used as feature vector. Calcified segments with high intensity values are separated from non-calcified ones with low intensity values. The classification is done on each CT slice separately by an SVM with a linear kernel. With the transformation matrix embedded in the CT slices, the points of detected calcification are projected into 3D space. The true predicted calcifications are shown in Fig. 14 along with the mesh that is generated out of the same CT data. The classification approach has been evaluated in a two-class (calcification, other) and three-class setting (calcification, aorta, other). This led to balanced accuracy results of 0.92 and 0.87 respectively.[82] For the two-class setting, from $1,526,990$ pixels belonging to the region of interest, only $6,222$ calcified pixels have not been detected (false negatives). The true positive rate amounts to 0.866, the false negative rate to 0.134, and the false positive rate to 0.017.

Figure 14. True positive calcification in 3D aorta mesh.[82]

Through appropriate registration or intra-operative modeling techniques the predicted calcification regions could then be updated estimating the intra-operative distribution.

5.5.2. *Branch detection*

Alternatively, risk prone areas can be measured directly, e.g. through intravascular ultrasound. In fact, IVUS is considered as the gold standard to detect calcifications[84] (see also Fig. 5(f)). Further, it is clinically known that plaques within the aorta are more likely to occur in close proximity to its branches.[85,86] Branch detection and automatic highlighting therefore could help increase the awareness of these risky areas. Previous approaches in branch detection in IVUS images and sequences have used shape-driven methods[87] and classification techniques.[88] However, these have mainly focused on the coronary arteries. IVUS images from 6 catheter pullback sequences were recorded and pre-processed. Classifiers were trained based on 5 of the pullback sequences. The remaining pullback was used as test set for evaluation. Features where obtained that characterize ellipses and circles, from respectively single best fitted and multiple fitted shapes. To fit multiple geometric shapes the Hough-Transform (HT) was employed. As classifier an $L1$-regularized SVM with linear kernel was applied. A Gaussian feature normalisation was found to deliver the best results with median balanced accuracy of ≈ 0.95 and worst balanced accuracy of 0.85. Additionally, efforts have been made to devise alternative branch detection methods, namely based on the lumen shape and the Radon transform(the projection of the image intensity along a radial line oriented at a specific angle). Initial results have shown better differentiation of images with branches than images without, especially over ellipse fitting approaches. The proposed method is computationally inexpensive and allows for real-time processing on IVUS images. Further work will be conducted to incorporate this information as the robotic catheter advances *towards* the aortic valve.

6. Skill analysis to evaluate and optimize catheter control

A direct translation of the available geometric, mechanic and anatomic information towards adequate catheter steering actions is difficult to achieve. The catheter invariably follows a complex path, whereby it is often impossible to avoid touching *some* risky areas. Experienced interventionalists have, through long years of training, learned to understand which areas can be contacted or, where contact cannot be avoided, what level of contact is acceptable. For an autonomous navigation system it is crucial that it possesses a similar navigation skill so that it can make the same trade-offs in a sensible and timely manner displaying an equivalent quality in decision making. Even under non-conventional working conditions e.g. when dealing with catheters with altered dexterity or offered additional navigation guidance, it is expected that such skill prevails. It is thus interesting to tap into the operator's brain and, while he/she accommodates to the new situation, maximally extract displayed navigation strategies. A 4DoF *teleoperation* system has been built to access this information. Whereas little research has been conducted to devise intuitive teleoperation catheter control schemes in the past and this research has thus its own merit, the teleoperation system additionally offers direct access to the operator input commands, which is of great use for objective skill assessment. As navigation strategies are assumed to vary as the task proceeds, it would be helpful to identify and attach the specific stages accross the traject. After presenting some first results on intuitive teleoperation control and guidance schemes in SubSec. 6.1, work on episode segmentation is presented in SubSec. 6.2 to help put the data into the right context. This information can then be fed to skill assesment techniques presented in SubSec. 6.3.

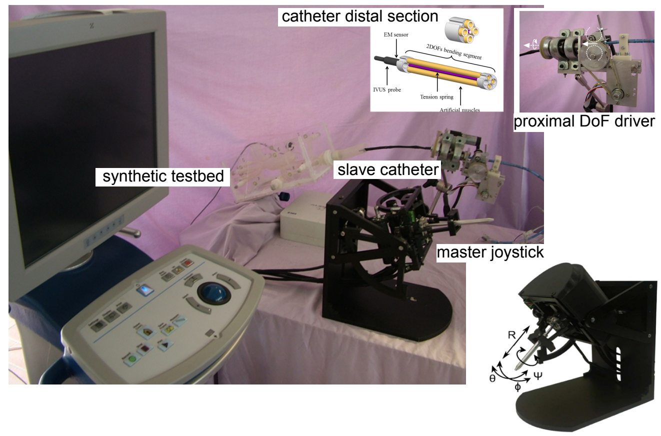

Figure 15. View on teleoperation setup built to investigate intuitive and efficient catheter steering strategies.[64,91]

6.1. *Teleoperation control and guidance*

Several works have dealt with catheter teleoperation control in the past. These works implement specific mappings between the different DoFs of the master robot and the slave robot, i.e. the robotic catheter.[55,89] However, little discussion took place as to which mapping is good to start with. Especially when it concerns steering complex multi-DoF catheters in highly dynamic environments this is an non-trivial question. Active catheters typically combine proximal with distal actuation DoFs, but, the reference frame in which the distal section is defined is constantly moving and rotating while the catheter is inserted. Tracking the motion of this distal section imposes a significant mental load upon the surgeon. Current *manual* interventions offer limited control over the catheter distal DoFs, but also existing commercial robotic systems are not designed for highly dynamic and coordinated control. Next to the unanswered question how to intuitively map user steering commands, the question arises how additional available information from models or intra-operative sensing can be presented to the user such that he/she can easily account for it and steer the catheter more reliably and with confidence through the aorta. To answer the first question, a teleoperation setup was built as depicted in Fig. 15. The system consists of a 2-DoF catheter driver that is used to control the proximal insertion and roll DoFs of various active catheters. The driver can be adjusted to accommodate different diameter catheters. An in-house built 4-DoF haptic joystick[90] steers the catheter DoFs. Although theoretically possible, clinicians advised against using the catheter roll-DoF as such motion would entail a large intrinsic contact with the vasculature, with consequent risks for plaque or calcium dislodgement. In first instance, three 3-DoF mappings $M1$, $M2$, $M3$ were tested and compared.[64] In $M1$, the so-called *direct joint-based mapping* the joystick linear, yaw and pitch DoFs are mapped to respectively the insertion (in rate control) and 2 pairs of antagonistic muscles, respectively. In $M2$, yaw and pitch joystick DoFs map to respectively the orientation of the distal bending plane (in which bending takes place) and bending amplitude. This requires proper coordinated control of the distal muscles. The rationale behind $M2$ is that the catheter curvature is more or less constant at the aortic arch. Crossing the arch would require thus less user input (little adjustment of bending amplitude). Mapping $M3$ helps taking into account catheter torsion. The torsion-induced rotation (roll) of the catheter is measured by a 6DoF EMT sensor embedded in the catheter tip. This rotation is then compensated for so that an angulation of the master joystick will correspond to a similar pitch or yaw angulation with respect to a fixed global reference frame.

Experiments were carried out by an expert endovascular surgeon on the setup depicted in Fig. 15. The employed catheter consisted of a single 60mm long distal section with 2 pairs of antagonistic fluidic muscles (thus offering 2 distal DoFs), following the layout of the catheter described in SubSec. 4.3. Multiple insertions were executed in a flexible aorta model. These first experiments, reported by Rosa *et al.*[64] showed that the user performed better with $M2$, both in terms of time to reach the aortic valve ($p = 0.03$), length of path ($p = 0.01$) and smoothness of the movements ($p = 0.03$). These experiments were next repeated with a larger population including novices and expert surgeons.[91] This time the in SubSec. 3.2 described VR environment was used. By shifting to VR, the catheter hardware could be spared. Experiments could be conducted faster and more repeatable as well. In these experiments, the better mappings $M1$ and $M2$ were compared and the effect of additional visual guidance, depicted in Fig.16 on steering performance was explored. From these experiments it was found that if visual guidance was provided the direct control mapping $M1$ was significantly outperforming the bending plane mapping $M2$ and this was the case irrespective of the expert level of the participants.[91]

6.2. *Episode segmentation*

Adequate navigation assistance is function of the specific context since control objectives and loads vary as the procedure progresses. For fully autonomous motion, the controller should understand and automatically adapt to the circumstances. A detailed analysis of the surgical workflow lies at the base of such cognitive system. Segmentation and identification of surgical episodes or tasks can alert the surgeon intra-operatively for difficult or risky areas within particular surgical steps. This can facilitate intra-operative catheter control and decision making, helping to safely navigate through a fragile and dynamic environment in the presence of large uncertainty about its properties. The analysis of the surgical tasks can further help to quantitatively evaluate surgical skill which migh vary depending on the specific episode within an entire procedure.

Thus far, workflow analysis has been extensively studied for minimally invasive procedures. Surgical tools,[92] visual and anatomical cues[93] as well as kinematic data[94] have been used to recognise surgical phases and actions. Our work has focused on the analysis of the workflow of cardiovascular procedures. More specifically, the workflow of the TAVI procedure was segmented by expert endovascular surgeons into 10 surgical tasks including the placement of a pacing catheter and a guidewire in the femoral vein, the introduction of an introducer sheath, the pre-dilation of the valve with a balloon, the delivery of the artificial valve and evaluation of the valve positioning. Given its central role within the procedure the 'Delivery of the aortic valve' (8^{th} task in line) was focused upon. This task has been further segmented into 6 sequential surgical gestures: (1) catheter pushed up the descending aorta, (2) catheter pushed around the aortic arch, (3) catheter pushed down the ascending aorta, (4) catheter pulled back in the ascending aorta, (5) catheter pulled back in the aortic arch, (6) catheter pulled back in the descending aorta.

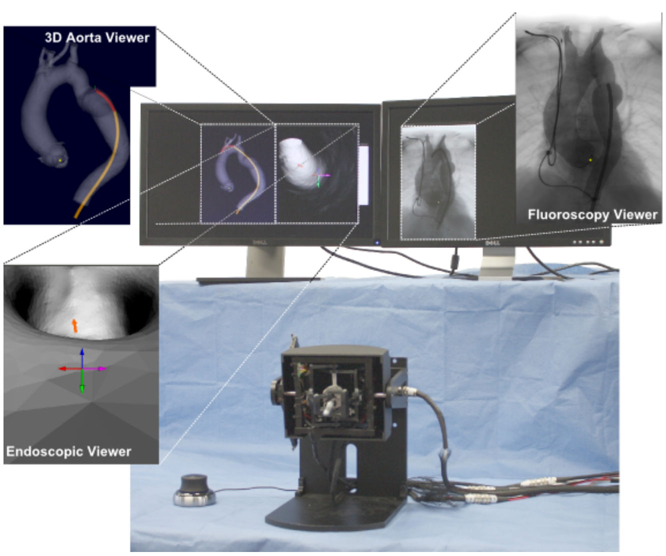

Figure 16. View upon setup of VR steering experiments. From pre- and intra-operative data, fluoroscopic, 3D and endoscopic views with additional guidance cues are being generated; arrows showing the relative location of the center-line or informing how joystick input commands map to catheter tip motion.[91]

An on-line approach for surgical gesture recognition has been developed.[95] Descriptive Curve Coding (DCC) was used to represent the 3D catheter motion with a set of motion words. To enable early recognition of partially-observed gestures, integral histograms of the motion words are generated to describe a surgical task. The 'dynamic bag-of-words' approach has been used to recognise surgical gestures, based on dynamic matching of integral histograms considering the sequential nature of gestures during surgical tasks. Detailed validation with phantom data has been performed. The performance of the method has been measured in terms of the mean accuracy, precision, sensitivity and specificity of the classification which was equal to 0.97, 0.91, 0.91 and 0.98, respectively over all the gestures. The results justify the potential clinical value of the technique.[95]

6.3. *Skill assessment*

Traditional methods for evaluating surgical expertise consist of written and oral examinations and expert supervision during experiments on cadavers, animals, inanimate models or virtual simulators. Assessment takes place using standardized grading scales (GRS) or checklists with an expert observing and assigning grades as the trainee executes a phantom operation. Supervised assessment is time-consuming and laborious, as well as subjective to a degree. This prohibits global standardization of technical expertise. Hereto, a detailed analysis of the state-of-the-art in endovascular surgical skills evaluation methods has been conducted.[96] Expert endovascular surgeons operate instruments in a smooth, steady way without jerky and unnecessary movements.[96] For autonomous operation, the robotic system must emulate the performance of an expert endovascular surgeon to deal with the challenges and risks of TAVI as outlined in SubSec. 2.1.

Under CASCADE, a novel approach to evaluate surgical skill has been developed. Empirical evidence suggests that the level of technical expertise is represented by the proper handling of surgical equipment in such a way that this is efficient and minimizes the risk for errors occurring.[97,98] In addition, virtually all established endovascular GRS and checklists contain criteria, that evaluate three key technical attributes, summarized as: 1) avoiding vessel wall damage with precise catheter manipulation, especially near delicate or sclerotic areas; 2) smooth timely catheter navigation without unnecessary movements; 3) efficient use of the imaging modalities and contrast agents. Inspired by this, we expanded skill assessment by focusing on 1) and 2) and hypothesized that quantitative measures extracted from analyzing medical images and tracking the instruments trajectory, combined appropriately, will contain the necessary information to discriminate experience levels.

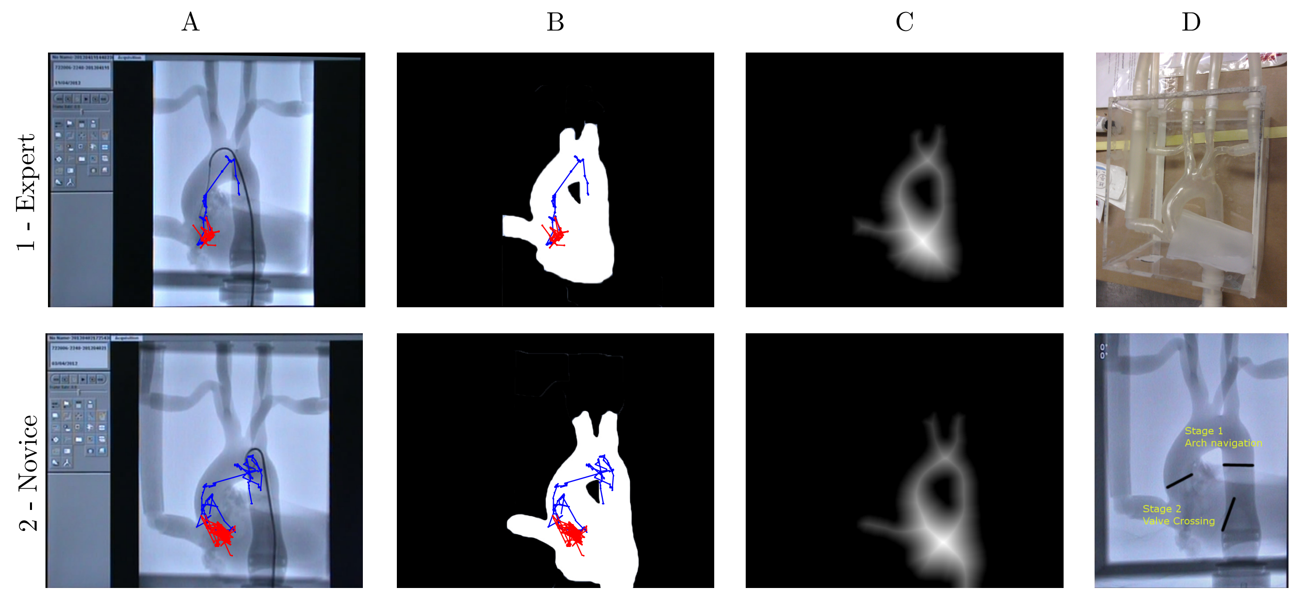

Figure 17. Image processing steps; Column A - Original fluoroscopy frames with tip position marked (blue - descending aorta, red - valve crossing); Column B - Binary image with segmented aorta model; Column C - Distance image shows the distance of each phantom model pixel (white) to the closest point on the vessel wall (first black pixel); higher intensity for higher distance. From 1,B and 2,B more efficient handling by the expert is seen; Column - D employed aorta model and boundaries of the 2 TAVI stages.

Experiments were carried out on an aorta silicon model (Fig. 17.D), with 12 endovascular surgeons of different experience (6 novices, 6 experts) using both conventional catheters and a robotic platform (Magellan™, Hansen Medical Inc.). Analysis was performed on recorded fluoroscopy video sequences. A semi-automated algorithm tracks the catheter/guidewire tip in the video frames. This information allows calculating a number of kinematic features (e.g. speed, acceleration, jerk). The aorta in the video frames was segmented and the distance to the vessel wall was computed to evaluate how safe the catheter is navigated with respect to adjacent vascular tissue. The processing pipeline and experimental testbed are illustrated in Fig. 17.

Total procedure time, average speed, average acceleration magnitude, dimensionless jerk and average distance (of the catheters tip and shape) to the vessel wall were metrics under study. As expected, the two groups demonstrated different procedure times especially when navigating the arch (p=0.008), with experts completing the tasks faster than novices. This was also demonstrated by higher values in average speed and acceleration in both TAVI stages (descending aorta cannulation, valve crossing). Smoothness was evaluated with the dimensionless jerk, a metric designed to be independent of duration and amplitude; experts, demonstrated smaller median values with the difference being statistically important (p=0.008) in stage 1. Ultimately, the features that demonstrated statistical significance served as inputs for k-means and expectation-maximisation clustering. Participants were classified according to their experience level with obtained level of accuracy being 83% - 91%;[99] results for EM clustering are shown in Fig. 18. The average distance to the wall did not demonstrate statistical significance among the two experience groups. However it was higher when the robotic system was used, particularly in the stage where the catheter was navigated through the aortic valve. Based on this, the robotic system appears to facilitate safer and more precise catheter manipulation.

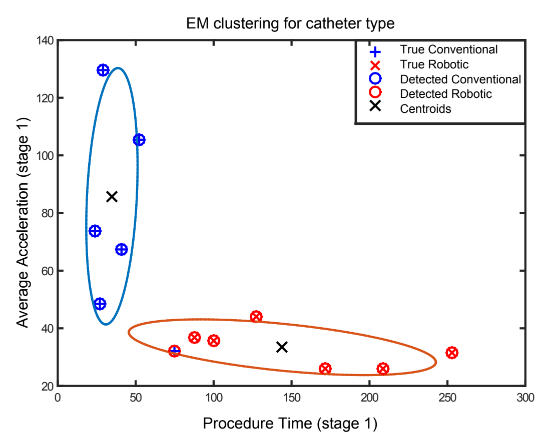

Figure 18. EM clustering using procedure time and average acceleration (11/12 - 91%).

7. Advanced Control

Equipped with new catheters, models and knowledge about skills, covered in Sec. 3-6, this section introduces a number of innovative control schemes directed at safe and effective autonomous catheter control. SubSec. 7.1 explores coordinated control of dynamic, compliant, deformable structures such as the catheter's distal tip. Subsec 7.2 and 7.3 address the control of entire catheters, following respectively minimum energy principles and machine learning techniques.

7.1. *Control of catheter distal section as a continuum robot*

Given the difference in bandwidth between the distal fluidic actuated tip and the rest of the catheter, in first instance, an approach was developed that focuses on the control of the distal part of the catheter. This part is treated as a continuum robot and abstraction is made of the catheter tail. Since the distal part has a large compliance this part can be modelled as a Cosserat rod so that deformations under externally applied loads can be accounted for. Fast computation schemes were developed to compute the Jacobian and Compliance matrices of the distal part.[100] Relying on this information position and force control schemes were derived. Hereto, the eTaSL/eTC, a constraint-based task formalism[101] that allows incorporating a plurality of objectives as constraints, was adopted.[102] Position and pivoting constraints are formulated to control the tip and the base of the distal section of the catheter (the catheter's centerline is made to pass through a fixed point in space). Force control was formulated via a velocity constraint. It was shown how such conversion could be done through the use of the forward kinematics and compliance of the distal segment and by measuring the force at the base of the distal section.[102]

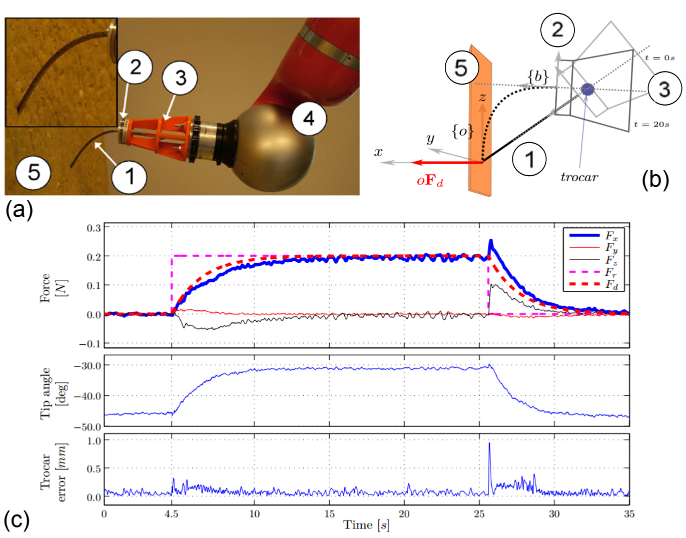

Figure 19. Experimental setup - (a) flexible link ①, representing the catheter distal section, mounted on ATI force sensor ②, attached to KUKA LWR ④ via a mounting stage ③; upper left: close-up of the flexible link; (b) upper right: sketch of setup before and after applying 0.2N step response on foamy structure ⑤; graph (c) the interaction as function of time: upper plot the interaction, middle graph the evolution of the tip orientation; bottom graph position error on base positioning constraint.[102]

Fig. 19 shows the experimental setup that was constructed to demonstrate the proposed approach. The system consists of a flexible link (representing the catheter's distal section) that is mounted via a force sensor (Nano 43, ATI, Apex, North Carolina) on a Light-Weight Robot (LWR), an industrial robot from KUKA AG (Augsburg, Germany). This system is controlled from an unloaded configuration at $t = 0\,s$ in contact with the wall (black line) to a loaded configuration ($t = 20\,s$, dashed black line), where it is commanded to apply a reference force of 0.2N upon a soft environment. At the same time the system is asked to maintain the center-line of the mounting frame at a fixed position. Such position could e.g. correspond to a non-risky location at the aortic wall which could serve as a safe *landing* zone for the base of the catheter's distal section. The graph shows that a desired force can be applied (bottom), while the position constraint can be held quite accurately (error shown in lower graph). It can be observed that the orientation of the catheter (which is not constrained) is largely affected because of the interaction. During valve placement the resulting deformation of the distal section is thus to be accounted for. Since integrating force sensing at the base of the distal section is not straightforward (reliable tactile skins are not available either), current investigations focus on reversing the method so that forward kinematics and compliance values can be obtained from shape information rather than from force measurements. The catheter tracking and environment reconstruction schemes presented in Sec. 5 could serve this purpose.

7.2. *Autonomous catheter control - minimum-energy approach*

Obtaining a sufficiently accurate kinematic map that is needed to apply the approach of SubSec. 7.1 for the entire robotic catheter requires detailed knowledge of *all* interactions between the robot and the vasculature. Such interactions are complex, intrinsically distributed and depend on the properties of both catheter and environment. In the absence of adequate tactile skins, an approach based on a quasi-static predictive model[37] was progressed. The method follows a minimum energy argumentation to predict changes of catheter shape upon varying robot/catheter actions. For a given input command the catheter will take in a new equilibrium configuration where the combined deformation energy of catheter and vessel wall is minimal. The input-output space[40] is probed by applying a number of *virtual* input commands and recording the corresponding outputs, i.e. catheter motions. From this the differential kinematics under the form of a Jacobian matrix is derived. The Jacobian's inverse is then used to estimate the appropriate input command for a targeted output motion. The proposed approach was verified in 2D and 3D models in VR. Fig. 20 shows a representative outcome of in-vitro experiments conducted on a 2-dimensional rigid mockup. Deviation from the target trajectory, here the vessel centerline, originated partially from limited accuracy of the shape sensing methods that were used here. The limited bending capabilities of the TactiCATh™catheter formed a second, more important factor. ote that a full insertion took 734s. The experiment was conducted in a two-dimensional environment since this made it easier to compute the error from the targeted path. Similar results (and computation times) were obtained from experiments conducted in the virtual reality simulator in 3D. In future work this approach is to be validated on synthetic 3D models as well.

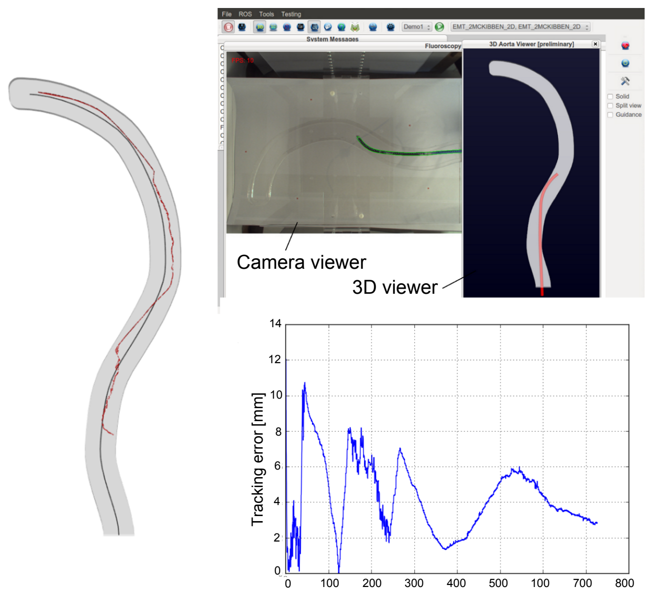

$e_H = 12.07mm \quad e_m \pm std = 4.30 \pm 2.03mm \quad e_{RMS} = 4.76mm$

Figure 20. Autonomous catheter navigation in rigid 2D mock-up; catheter with single bending segment and bending angle limited to [−55°;50°]. [right up] View on CASCADE platform. The camera viewer displays the detected catheter contours and centerline (green lines). The catheter centerline is registered to the mesh coordinate frame and sent to the minimum energy model and associated controller. The registered catheter shape is visible as red tube in 3D viewer; [left] tip position (red line) and target path (black line); [bottom] Tracking errors: Hausdorff error, mean error, standard deviation, RMS error respectively: e_h=12.073mm, $e_m \pm$ std=4.0 ± 2.032 mm and e_{rms}=4.756mm.

7.3. *Autonomous catheter control: a data-driven approach*

Machine learning techniques can be adopted to learn the input-output behaviour of the catheter inside vessels of artificial mock-ups directly from the data. A data-based catheter steering method[103, 104] was proposed and tested in a 2D deformable aorta mock-up. Whereas the methods have been applied on a cable-driven catheter TactiCath™, the proposed approaches are more general and transfer also to highermentioned McKibben-based catheters.

The catheters are modelled using joint probability densities, which are represented by mixture of Gaussians. A Dynamic Gaussian Mixture Model (DGMM) served for probabilistic representation. DGMM is the extended version of the standard Gaussian Mixture Model (GMM), which allows dynamic variation of the number of Gaussian components in the model.[103] This helps capturing multiple relationships among variables of the catheter model. Additionally, the online methods implemented in DGMM allow updating the model incrementally as more data is acquired, making DGMM a good candidate for a system that learns continuously. During training of the joint probability distribution, different features of the catheter such as the catheter tip position, the catheter shape and the bending angle are captured and used as input data to the model. The trained model and steering approach are tested by a centerline following experiment in a 2D deformable aorta mock-up. The detected features of the catheter and the experimental results are shown in Fig. 21. The mean Euclidean distance of the catheter tip is 7.63 mm. Due to friction and hardware limitations the error rises up to 12.2 mm at specific locations along the trajectory. Currently work is ongoing to train the McKibben-based catheter to navigate through the 3D deformable model.

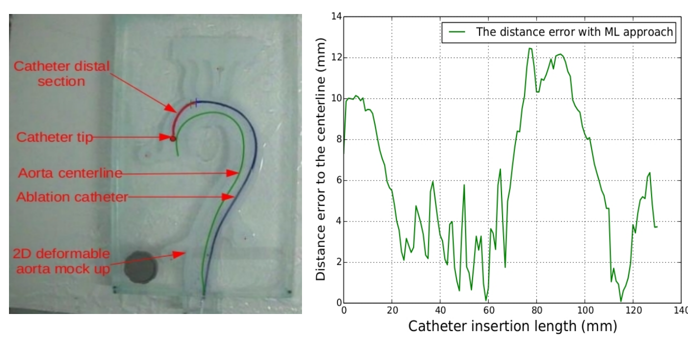

Figure 21. In-vitro experiment of autonomous catheter navigation in a 2D deformable mock-up, with single bending segment and bending angle limited to [15°;70°]. [left] The camera image displays the detected catheter distal section (red line), catheter tip (red dot), catheter body (blue line) and aorta centerline (green line); [right] The tracking error is calculated between the catheter tip and the aorta centerline after each steering action.

8. Conclusions and future work

Advances in miniaturized surgical instrumentation and control are key to less demanding and safer medical interventions. This paper reports on the progress that has been made within the EU-funded CASCADE project; progress in terms of a number of key technologies that lead to autonomous catheter steering. Novel catheters actuated by fluidic muscles have been built showing operational bandwidths higher than 8Hz and excellent controllability. Equiped with a combination of proprio- and exteroceptive sensors these catheters allow estimating the own shape, but also reconstruction of the surrounding vasculature. Relying on these embedded sensors, a fully automatic registration method is proposed. Without requiring any user input the method automatically registers a pre-operative mesh while the catheter is advanced through the vessel. New methods to estimate the 3D catheter shape relying on EMT and fusing EMT with fluoroscopy have been presented. With rms-errors in VR below 3mm, validation in a clinical setting is desirable. SCEM and SCEM+ are two algorithms that allow intra-operative vessel reconstruction based on IVUS and EMT. These algorithms offer a.o. intra-operative updates of the deformed vessel centerline, which can then be used to e.g. update mechanical vessel models. From the developed FEM methods it becomes then possible to estimate detailed stress levels during the intervention and re-plan trajectories if needed. Further efforts on collision detection are needed to actually get this functionality available in real-time. An updated vessel representation can further help estimating the exact location of risk prone areas in the vessel. Machine learning methods were developed to automatically detect calcification in pre-operative CT, or relying on IVUS, to detect the location of side branches. A series of experiments was set up to get a grasp of steering skill that is displayed by expert surgeons. From teleoperation experiments and study of fluoroscopic images during actual interventions the characteristics of catheter handling were analysed. A technique was developed to automatically identify the different episodes during a surgical intervention. Further study is needed to quantify episode-specific characteristics. Finally, new control algorithms were developed to control the distal catheter tip with a constraint-based approach, or to control the entire catheter based on minimum-energy or machine learning methods. Whereas the force control performance of the former was demonstrated when interacting on a 3D soft environment, latter methods were only demonstrated on 2D rigid and deformable mockups. Currently experiments on a 3D setup with the novel catheters are being conducted.

The route proposed by CASCADE is one that reduces the invasiveness of catheter-based procedures. Not only by limiting the dependency on damaging imaging techniques, or shortening the execution time, but also by offering better control over the interaction between catheter and the vessel. Latter is necessary to reduce risks for calcium or plaque dislogement and puncturing of the vessel. This calls for detailed up-to-date models of the catheter and the vessel and superior control over the catheter itself. While fully autonomous catheter steering is neither feasible on the mid-term, nor desirable, progress presented in this paper on some key technologies could prove useful on a shorter term. Further efforts will therefore be focused on verification and validation of the individual and combined technologies in more realistic settings. It is believed that also the newly developed synthetic and VR testbeds could find good use to train surgeons or validate new instruments. We are currently looking at setting up hybrid testbeds where information from VR augments the synthetic testbeds offering increased levels of immersiveness and realism, establishing an even better environment for prototyping and validation.

Acknowledgments

Research funded by the European Commission's 7th Framework Programme FP7-ICT - under grant agreement No601021, EU project CASCADE. The authors wish to express their gratitude towards Volcano Corporation (Volcano Europe) for making their ultrasound system available for the purpose of the here conducted research.

Bibliography

[1] M. Nichols, N. Townsend, P. Scarborough, and M. Rayner, "Cardiovascular disease in europe 2014: epidemiological update," *European heart journal*, vol. 35, no. 42, pp. 2950–2959, 2014.

[2] D. Mozaffarian, E. J. Benjamin, A. S. Go, D. K. Arnett, M. J. Blaha, M. Cushman, S. de Ferranti, J.-P. Despres, H. J. Fullerton, V. J. Howard *et al.*, "Heart disease and stroke statistics-2015 update: a report from the american heart association." *Circulation*, vol. 131, no. 4, p. e29, 2015.

[3] M. Mirabel, B. Iung, G. Baron, D. Messika-Zeitoun, D. Detaint *et al.*, "What are the characteristics of patients with severe, symptomatic, mitral regurgitation who are denied surgery?" *Eur Heart Journal*, vol. 28, no. 11, pp. 1358–1365, Mar 2007.

[4] M. B. Leon, C. R. Smith, M. Mack, D. C. Miller, J. W. Moses *et al.*, "Transcatheter aortic-valve implantation for aortic stenosis in patients who cannot undergo surgery," *New England Journal of Medicine*, vol. 363, no. 17, pp. 1597–1607, 2010.

[5] C. R. Smith, M. B. Leon, M. J. Mack, D. C. Miller, J. W. Moses, L. G. Svensson, E. M. Tuzcu, J. G. Webb, G. P. Fontana, R. R. Makkar *et al.*, "Transcatheter versus surgical aortic-valve replacement in high-risk patients," *New England Journal of Medicine*, vol. 364, no. 23, pp. 2187–2198, 2011.

[6] R. R. Makkar, G. P. Fontana, H. Jilaihawi, S. Kapadia, A. D. Pichard *et al.*, "Transcatheter aortic-valve replacement for inoperable severe aortic stenosis," *New England Journal of Medicine*, vol. 366, no. 18, pp. 1696–1704, 2012.

[7] L. Kohn, J. Corrigan, and M. Donaldson, *To err is human: building a safer health system.* Washington: National Academy Press, 2000.

[8] R. Morena, L. Calvo, P. Salinas, D. Dobarro, J. Santiago, A. Sanchez-Recalde *et al.*, "Causes of peri-operative mortality after transcatheter aortic valve implantation: A pooled analysis of 12 studies and 1,223 patients," *J INVASIVE CARDIOL*, vol. 23, pp. 180–184, 2011.

[9] G. Tarantini, V. Gasparetto, M. Napodano, C. Fraccaro, G. Gerosa, and G. Isabella, "Valvular leak after transcatheter aortic valve implantation: a clinician update on epidemiology, pathophysiology and clinical implications," *American journal of cardiovascular disease*, vol. 1, no. 3, p. 312, 2011.

[10] A. Ghanem, A. Müller, C. P. Nähle, J. Kocurek, N. Werner, C. Hammerstingl, H. H. Schild, J. O. Schwab, F. Mellert, R. Fimmers *et al.*, "Risk and fate of cerebral embolism after transfemoral aortic valve implantation: a prospective pilot study with diffusion-weighted magnetic resonance imaging," *Journal of the American College of Cardiology*, vol. 55, no. 14, pp. 1427–1432, 2010.

[11] Q. M. de Ruiter, F. L. Moll, and J. A. van Herwaarden, "Current state in tracking and robotic navigation systems for application in endovascular aortic aneurysm repair," *Journal of Vascular Surgery*, vol. 61, no. 1, pp. 256 – 264, 2015.

[12] O. De Backer, N. Piazza, S. Banai, G. Lutter, F. Maisano, H. Herrmann, O. Franzen, and L. Sondergaard, "Percutaneous transcatheter mitral valve replacement: An overview of devices in preclinical and early clinical evaluation," *Circulation: Cardiovascular Interv.*, vol. 7, no. 3, pp. 400–409, 2014.

[13] W. Zhang, N. Jia, J. Su, J. Lin, F. Peng, and W. Niu, "The comparison between robotic and manual ablations in the treatment of atrial fibrillation: A systematic review and meta-analysis," *PloS one*, vol. 9, no. 5, p. e96331, 2014.

[14] D. Bach, J. Radeva, H. Birnbaum, A.-A. Fournier, and E. Tuttle, "Prevalence, referral patterns, testing, and surgery in aortic valve disease: leaving women and elderly patients behind?" *The Journal of heart valve disease*, vol. 16, no. 4, pp. 362–369, 2007.

[15] C. M. Otto, "Timing of aortic valve surgery," *Heart*, vol. 84, no. 2, pp. 211–218, 2000.

[16] B. Iung, G. Baron, E. G. Butchart, F. Delahaye, C. Gohlke-Bärwolf, O. W. Levang, P. Tornos, J.-L. Vanoverschelde, F. Vermeer, E. Boersma *et al.*, "A prospective survey of patients with valvular heart disease in europe: The euro heart survey on valvular heart disease," *European heart journal*, vol. 24, no. 13, pp. 1231–1243, 2003.

[17] E. Charlson, A. T. Legedza, and M. B. Hamel, "Decision-making and outcomes in severe symptomatic aortic stenosis," *Journal of Heart Valve Disease*, vol. 15, no. 3, p. 312, 2006.

[18] A. Kasel, S. Cassese, A. Leber, W. von Scheidt, and A. Kastrati, "Fluoroscopy-guided aortic root imaging for TAVR: 'Follow the Right Cusp' rule," *JACC: Cardiov. Imag.*, vol. 6, no. 2, pp. 274 – 275, 2013.

[19] J. Plotkin, R. Siegel, and R. Beigel, "Plaque disruption during transcatheter aortic valve replacement," *Eur. Heart J. Cardiovasc. Imaging*, vol. 15, no. 1, pp. 117–117, Jan 2014.

[20] A. Aminian, J. Lalmand, and B. El Nakadi, "Perforation of the descending thoracic aorta during transcatheter aortic valve implantation (tavi): An unexpected and dramatic procedural complication," *Catheterization and Cardiovascular Interventions*, vol. 77, no. 7, pp. 1076–1078, 2011.

[21] J. Webb, S. Pasupati, L. Achtem, and C. Thompson, "Rapid pacing to facilitate transcatheter prosthetic heart valve implantation," *Catheterization and cardiovascular interv.*, vol. 68, no. 2, pp. 199–204, 2006.

[22] J. Bonatti, G. Vetrovec, C. Riga, O. Wazni, and P. Stadler, "Robotic technology in cardiovascular medicine," *Nature Reviews Cardiology*, vol. 11, no. 5, pp. 266–275, 2014.

[23] H. Rafii-Tari, C. J. Payne, and G.-Z. Yang, "Current and emerging robot-assisted endovascular catheterization technologies: A review," *Annals of biomedical engineering*, vol. 42, no. 4, pp. 697–715, 2014.

[24] M. Anselmino and F. Gaita, "Unresolved issues in transcatheter atrial fibrillation ablation: silent cerebrovascular ischemias," *Journal of cardiovascular electrophysiology*, vol. 24, no. 2, pp. 129–131, 2013.

[25] S. G. Yuen, S. B. Kesner, N. V. Vasilyev, P. J. Del Nido, and R. D. Howe, "3d ultrasound-guided motion compensation system for beating heart mitral valve repair," in *Medical Image Computing and Computer-Assisted Intervention–MICCAI 2008.* Springer, 2008, pp. 711–719.

[26] V. Meiser and D. Seatovic, "System integration: A comparison of the scath and the cascade system architecture," in *Proceedings of the 3rd Joint Workshop on New Technologies for Computer - Robot Assisted Surgery*, 11-13 Sep. 2013 2013, pp. 130–133.

[27] M. Quigley, K. Conley, B. Gerkey, J. Faust, T. Foote, J. Leibs, R. Wheeler, and A. Y. Ng, "Ros: an open-source robot operating system," in *ICRA workshop on open source software*, vol. 3, no. 3.2, 2009, p. 5.

[28] H. Bruyninckx, P. Soetens, and B. Koninckx, "The real-time motion control core of the orocos project," in *Robotics and Automation, 2003. Proceedings. ICRA'03. IEEE International Conference on*, vol. 2. IEEE, 2003, pp. 2766–2771.

[29] V. Luboz, R. Blazewski, D. Gould, and F. Bello, "Real-time guidewire simulation in complex vascular models," *Vis. Comput.*, vol. 25, pp. 827–834, 2009.

[30] F. Wang, L. Duratti, E. Samur, U. Spaelter, and H. Bleuler, "A computer-based real-time simulation of interventional radiology." in *Conf Proc IEEE Eng Med Biol Soc*, 2007.

[31] S. Cotin, C. Duriez, J. Lenoir, P. Neumann, and S. Dawson, "New approaches to catheter navigation for interventional radiology simulation," in *Proceedings of the 8th international conference on Medical image computing and computer-assisted intervention - Volume Part II*, ser. MICCAI'05. Berlin, Heidelberg: Springer-Verlag, 2005, pp. 534–542.

[32] S. Li, J. Qin, J. Gao, Y.-P. Chui, and P.-A. Heng, "A novel fem-based numerical solver for interactive catheter simulation in virtual catheterization," *Journal of Biomedical Imaging*, vol. 2011, p. 3:3, 2011.

[33] W. Tang, P. Lagadec, D. Gould, T. Wan, J. Zhai, and T. How, "A realistic elastic rod model for real-time simulation of minimally invasive vascular interventions," *Vis. Comput.*, vol. 26, no. 9, pp. 1157–1165, 2010.

[34] M. Konings, E. Kraats, T. Alderliesten, and

W. Niessen, “Analytical guide wire motion algorithm for simulation of endovascular interventions,” *Medical and Biological Engineering and Computing*, vol. 41, no. 6, pp. 689–700, 2003.

[35] T. Alderliesten, M. Konings, and W. Niessen, “Simulation of minimally invasive vascular inventions for training purposes,” *Comput Aided Surg*, vol. 9, no. 1–2, pp. 3–15, 2004.

[36] ——, “Robustness and complexity of a minimally invasive vascular intervention simulation system,” *Medical Physics*, vol. 33, no. 12, pp. 4758–4769, 2006.

[37] T. Alderliesten, P. A. N. Bosman, and W. Niessen, “Towards a real-time minimally-invasive vascular intervention simulation system,” *IEEE Trans. on Medical Imaging*, vol. 26, no. 1, pp. 128–132, 2007.

[38] T. Alderliesten, M. Konings, and W. Niessen, “Modeling friction, intrinsic curvature, and rotation of guide wires for simulation of minimally invasive vascular interventions,” *Biomedical Engineering, IEEE Trans. on*, vol. 54, no. 1, pp. 29–38, 2007.

[39] P. Tran, A. Devreker, G. Smoljkic, H. De Praetere, E. Vander Poorten, and J. Vander Sloten, “Patient-specific design of multi-component steerable catheters,” in *Proc. of 3rd Joint Workshop on New Technologies for Computer - Robot Assisted Surgery*, 2013, pp. 37–40.

[40] P. Tran, E. Vander Poorten, G. Smoljkic, C. Gruijthuijsen, P. Herijgers, D. Reynaerts, and J. Vander Sloten, “Manipulability of robotic catheters,” in *Proc. 4th Joint Workshop on New Technol. for Comp. - Robot Assisted Surgery*, 2014, pp. 135–138.

[41] A. Tibebu, B. Yu, Y. Kassahun, E. Vander Poorten, and P. Tran, “Towards autonomous robotic catheter navigation using reinforcement learning,” in *Proc. 4th Joint Workshop on New Technologies for Computer - Robot Assisted Surgery*, 2014, pp. 163–166.

[42] W. Russell, R. Burch, and C. Hume, “The principles of humane experimental technique,” 1959.

[43] M. Kvasnytsia, N. Famaey, M. Böhm, and E. Verhoelst, “Patient specific vascular benchtop models for development and validation of medical devices for minimally invasive procedures,” *Journal of Medical Robotics Research*, 2016 (submitted).

[44] G. Biglino, P. Verschueren, R. Zegels, A. M. Taylor, and S. Schievano, “Rapid prototyping compliant arterial phantoms for in-vitro studies and device testing,” *J Cardiovasc Magn Reson*, vol. 15, no. 2, pp. 1–7, 2013.

[45] B. A. Childers, D. K. Gifford, R. G. Duncan, M. T. Raum, M. E. Vercellino, and M. E. Froggatt, “Fiber optic position and shape sensing device and method relating thereto,” Aug. 24 2010, uS Patent 7,781,724.

[46] V. Duindam, G. M. Prisco, T. W. Rogers, and J. R. Steger, “Method and system to sense relative partial-pose information using a shape sensor,” Jul. 16 2013, US Patent 8,488,130.

[47] C. Shi, S. Giannarou, S. Lee, and G. Yang, “Simultaneous catheter and environment modeling for transcatheter aortic valve implantation,” in *Proceedings of IEEE/RSJ International Conference on Intelligent Robots and Systems (IROS)*, 2014, pp. 2024–2029.

[48] A. Franz, T. Haidegger, W. Birkfellner, K. Cleary, T. Peters, and L. Maier-Hein, “Electromagnetic tracking in medicine - a review of technology, validation, and applications,” *Medical Imaging, IEEE Transactions on*, no. 8, pp. 1702–1725, Aug 2014.

[49] K. S. Rathod, S. M. Hamshere, D. A. Jones, and A. Mathur, “Intravascular ultrasound versus optical coherence tomography for coronary artery imaging–apples and oranges,” *Interventional Cardiology Review*, vol. 10, pp. 8–15, 2015.

[50] Y. Honda and P. J. Fitzgerald, “Frontiers in intravascular imaging technologies,” *Circulation*, vol. 117, no. 15, pp. 2024–2037, 2008.

[51] E. Tammam, “Intravascular magnetic resonance imaging (ivmri): Technology survey,” in *Int. Conf. on Information Technology: Research and Education*. IEEE, 2006, pp. 39–44.

[52] S. Nazarian, B. Knight, T. Dickfeld, M. Zviman, V. Jayanti, D. Amundson, J. Hanlin, J. Castleberry, M. Smith, L. Blankenship, H. Halperin, T. B. Ferguson, Jr, and R. Berger, “Direct visualization of coronary sinus ostium and branches with a flexible steerable fiberoptic infrared endoscope.” *Heart Rhythm*, vol. 2, no. 8, pp. 844–848, Aug 2005.

[53] C. Tekes, T. Xu, and F. Degertekin, “Improved flivus imaging with low voltage single-chip cmut-on-cmos array using temporally coded excitation,” in *Ultrasonics Symposium (IUS), 2014 IEEE International*, Sept 2014, pp. 1308–1311.

[54] G. Srimathveeravalli, T. Kesavadas, and X. Li, “Design and fabrication of a robotic mechanism for remote steering and positioning of interventional devices,” *Int. J. Medical Robotics and Computer Assisted Surgery*, vol. 6, no. 2, pp. 160–170, 2010.

[55] S. Kesner and R. Howe, “Position control of motion compensation cardiac catheters,” *Robotics, IEEE Transactions on*, vol. 27, no. 6, pp. 1045–1055, 2011.

[56] ——, “Robotic catheter cardiac ablation combining ultrasound guidance and force control,” *The International Journal of Robotics Research*, 2014.

[57] G. Vrooijink, T. Ellenbroek, P. Breedveld, J. Grandjean, and S. Misra, “A preliminary study on using a robotically-actuated delivery sheath (rads) for transapical aortic valve implantation,” in *IEEE Int. Conf. Robot. Autom.*, 2014, pp. 4380–4386.

[58] T. Fukuda, S. Guo, K. Kosuge, F. Arai, M. Negoro, and K. Nakabayashi, “Micro active catheter system with multi degrees of freedom,” in *Robotics and Automation, 1994. Proceedings., 1994 IEEE International Conference on*, may 1994, pp. 2290 –2295 vol.3.

[59] J. Jayender, R. V. Patel, and S. Nikumb, “Robot-assisted active catheter insertion: algorithms and experiments,” *The International Journal of Robotics Research*, vol. 28, no. 9, pp. 1101–1117, 2009.

[60] Y. Fu, H. Liu, W. Huang, S. Wang, and Z. Liang,

"Steerable catheters in minimally invasive vascular surgery," *The International Journal of Medical Robotics and Computer Assisted Surgery*, vol. 5, no. 4, pp. 381–391, 2009.

[61] K. Ikuta, H. Ichikawa, and K. Suzuki, "Safety-active catheter with multiple-segments driven by micro-hydraulic actuators," in *Medical Image Computing and Computer-Assisted Intervention MICCAI 2002*, ser. Lecture Notes in Computer Science, T. Dohi and R. Kikinis, Eds. Springer Berlin Heidelberg, 2002, vol. 2488, pp. 182–191.

[62] A. Devreker, E. Vander Poorten, P. Tran, H. De Praetere, P. Herijgers, J. Vander Sloten, and D. Reynaerts, "Towards fluidic actuation for catheter-based interventions," in *Proceedings Actuator 2014*, Bremen, Germany, 2014, pp. 173–176.

[63] A. Devreker, B. Rosa, A. Desjardins, E. Alles, L. Garcia-Peraza, E. Maneas, D. Stoyanov, T. Vercauteren, A. David, J. Deprest, S. Ourselin, D. Reynaerts, and E. Vander Poorten, "Fluidic actuation for intra-operative in situ imaging," in *Intelligent Robots and Systems, 2015. (IROS 2015). Proceedings. 2015 IEEE/RSJ International Conference on*, 2015, p. accepted for publication.

[64] B. Rosa, A. Devreker, H. De Praetere, C. Gruijthuijsen, S. Portoles-Diez, A. Gijbels, D. Reynaerts, P. Herijgers, J. Vander Sloten, and E. Vander Poorten, "Intuitive teleoperation of active catheters for endovascular surgery," in *Intelligent Robots and Systems, 2015. (IROS 2015). Proceedings. 2015 IEEE/RSJ International Conference on*, 2015, p. accepted for publication.

[65] J. Sra and S. Ratnakumar, "Cardiac image registration of the left atrium and pulmonary veins," *Heart Rhythm*, vol. 5, no. 4, pp. 609 – 617, 2008.

[66] Z. J. Malchano, P. Neuzil, R. C. Cury, G. Holmvang, J. Weichet *et al.*, "Integration of cardiac ct/mr imaging with three-dimensional electroanatomical mapping to guide catheter manipulation in the left atrium: Implications for catheter ablation of atrial fibrillation," *J. of Cardiovasc. Electrophysiol.*, vol. 17, no. 11, pp. 1221–1229, 2006.

[67] J. Dong, T. Dickfeld, D. Dalal, A. Cheema, C. R. Vasamreddy *et al.*, "Initial experience in the use of integrated electroanatomic mapping with three-dimensional mr/ct images to guide catheter ablation of atrial fibrillation," *J. of Cardiovasc. Electrophysiol.*, vol. 17, no. 5, pp. 459–466, 2006.

[68] T. W. G. Carrell, B. Modarai, J. R. I. Brown, and G. P. Penney, "Feasibility and limitations of an automated 2d-3d rigid image registration system for complex endovascular aortic procedures," *Journal of Endovascular Therapy*, vol. 17, no. 4, pp. 527–533, 2010.

[69] H. Zhong, T. Kanade, and D. Schwartzman, "Virtual touch: An efficient registration method for catheter navigation in left atrium," in *Medical Image Computing and Computer-Assisted Intervention*, 2006, pp. 437–444.

[70] C. Gruijthuijsen, B. Rosa, P.-T. Tran, J. Vander Sloten, E. Vander Poorten, and D. Reynaerts, "An automatic registration method for radiation-free catheter navigation guidance," *Journal of Medical Robotics Research*, 2016 (submitted).

[71] C. Papazov and D. Burschka, "Stochastic global optimization for robust point set registration," *Computer Vision and Image Understanding*, vol. 115, no. 12, pp. 1598 – 1609, 2011.

[72] P. Chang, A. Rolls, C. Riga, C. Bicknell, and D. Stoyanov, "A b-spline tube model for catheter and guidewire tracking," in *Proceedings of the 4th Joint Workshop on New Technologies for Computer - Robot Assisted Surgery*, 2014, pp. 41–43.

[73] C. Bibby and I. Reid, "Robust real-time visual tracking using pixel-wise posteriors," in *European Conference on Computer Vision*, 2008, pp. 831–844.

[74] E. Lugez, H. Sadjadi, D. Pichora, R. Ellis *et al.*, "Electromagnetic tracking in surgical and interventional environments: usability study," *Int. Journal of Computer Assisted Radiology and Surgery*, 2014.

[75] A. M. Franz, T. Haidegger, W. Birkfellner, K. Cleary *et al.*, "Electromagnetic tracking in medicine -A review of technology, validation, and applications," *IEEE Transactions on Medical Imaging*, vol. 33, no. 8, pp. 1702–1725, 2014.

[76] Z. Liang, S. Giannarou, S.-L. Lee, and G.-Z. Yang, "Scem+ : Real-time robust simultaneous catheter and environment modelling for endovascular navigation," in *IEEE RA-L*, 2016 (submitted).

[77] R. Tilz, K. Chun, A. Metzner, A. Burchard, E. Wissner, B. Koektuerk, M. Konstantinidou, D. Nuyens, T. De Potter, K. Neven, A. Furnkranz, F. Ouyang, and B. Schmidt, "Unexpected high incidence of esophageal injury following pulmonary vein isolation using robotic navigation," *Journ. of Cardiovascular Electrophysiology*, vol. 21, no. 8, pp. 853–8, August 2010.

[78] J. Gregson, A. Sheffer, and E. Zhang, "All-hex mesh generation via volumetric polycube deformation," in *Computer graphics forum*, vol. 30, no. 5. Wiley Online Library, 2011, pp. 1407–1416.

[79] K. Miller, G. Joldes, D. Lance, and A. Wittek, "Total lagrangian explicit dynamics finite element algorithm for computing soft tissue deformation," *Communications in Numerical Methods in Engineering*, vol. 23, no. August 2006, pp. 121–134, 2007.

[80] V. Strbac, J. V. Sloten, and N. Famaey, "Analyzing the potential of gpgpus for real-time explicit finite element analysis of soft tissue deformation using cuda," *Finite Elements in Analysis and Design*, vol. 105, pp. 79 – 89, 2015.

[81] T. C. Gasser, R. W. Ogden, and G. A. Holzapfel, "Hyperelastic modelling of arterial layers with distributed collagen fibre orientations," *Journal of the royal society interface*, vol. 3, no. 6, pp. 15–35, 2006.

[82] C. Rauch, B. Yu, A. T. Tibebu, and J. H. Metzen, "Detection and avoidance of aortic calcification in

minimal invasive catheter surgery," *Journal of Medical Robotics Research*, 2016, submitted.

[83] R. Achanta, A. Shaji, K. Smith, A. Lucchi, P. Fua, and S. Ssstrunk, "SLIC Superpixels Compared to State-of-the-art Superpixel Methods," *IEEE Transactions on Pattern Analysis and Machine Intelligence*, 2012.

[84] A. H. Ben, K. Bouzouita, I. Hamdi, A. Mokaddem, A. Y. Ben, and M. Boujnah, "Comparison of coronary calcifications detection by angiogram versus intravascular ultrasound." *La Tunisie medicale*, vol. 91, no. 3, pp. 196–199, 2013.

[85] G. D. Giannoglou, A. P. Antoniadis, K. C. Koskinas, and Y. S. Chatzizisis, "Flow and atherosclerosis in coronary bifurcations," *EuroIntervention : journal of EuroPCR in collaboration with Working Group on Interventional Cardiology of the European Society of Cardiology*, vol. 6 Suppl J, pp. J16–23, 2010.

[86] O. Arjmandi-Tash, S. E. Razavi, and R. Zanbouri, "Possibility of atherosclerosis in an arterial bifurcation model," *BioImpacts: BI*, vol. 1, no. 4, p. 225, 2011.

[87] G. Unal, S. Bucher, S. Carlier, G. Slabaugh, F. Tong, and K. Tanaka, "Shape-driven segmentation of the arterial wall in intravascular ultrasound images," in *IEEE Transactions on Information Technology in Biomedicine*, vol. 12, 2008, pp. 335–347.

[88] M. Alberti, S. Balocco, C. Gatta, F. Ciompi, O. Pujol, J. Silva, X. Carrillo, and P. Radeva, "Automatic bifurcation detection in coronary ivus sequences," in *IEEE Transactions on Biomedical Engineering*, vol. 59, 2012, pp. 1022–1031.

[89] J. Jayender and R. Patel, "Wave variables based bilateral teleoperation of an active catheter," in *Biomedical Robotics and Biomechatronics, 2008. BioRob 2008. 2nd IEEE RAS EMBS International Conference on*, Oct 2008, pp. 27–32.

[90] A. Gijbels, E. Vander Poorten, P. Stalmans, H. Van Brussel, and D. Reynaerts, "Design of a teleoperated robotic system for retinal surgery," in *IEEE International Conference on Robotics and Automation*, 2014.

[91] A. Devreker, P.-T. Tran, H. Rosa, B.and De Praetere, N. Häni, N. Famaey, D. Seatovic, P. Herijgers, J. Vander Sloten, D. Reynaerts, and E. Vander Poorten, "Intuitive control strategies for teleoperation of active catheters in endovascular surgery," *Journal of Medical Robotics Research*, 2016 (submitted).

[92] F. Lalys, D. Bouget, L. Riffaud, and P. Jannin, "Automatic knowledge-based recognition of low-level tasks in ophthalmological procedures," *International Journal of Computer Assisted Radiology and Surgery*, vol. 8, no. 1, pp. 39–49, 2013.

[93] L. Zappella, B. Bejar, G. Hager, and R. Vidal, "Surgical gesture classification from video and kinematic data," *Medical Image Analysis*, vol. 17, no. 7, pp. 732–745, 2013.

[94] B. Varadarajan, "Learning and inference algorithms for dynamical system models of dextrous motion," Ph.D. dissertation, The Johns Hopkins University, 2011.

[95] S. Giannarou, C. Gruijthuijsen, and G. Yang, "Modeling and recognition of ongoing surgical gestures in tavi procedures," in *Workshop on Modeling and Monitoring of Computer Assisted Interventions (M2CAI), Int. Conf. on Medical Image Computing and Computer Assisted Intervention (MICCAI)*, 2014.

[96] E. Mazomenos, P.-L. Chang, A. Rolls, D. Hawkes, A. Desjardins, C. Bicknell, E. Vander Poorten, C. Riga, and D. Stoyanov, "A survey on the current status and future challenges towards objective skills assessment in endovascular surgery," *Journal of Medical Robotics Research*, 2016 (submitted).

[97] C. Reiley, H. Lin, D. Yuh, and G. Hager, "Review of methods for objective surgical skill evaluation," *Surgical Endoscopy*, vol. 25, pp. 356–366, 2011.

[98] S. K. Neequaye, R. Aggarwal, I. Van Herzeele, A. Darzi, and N. J. Cheshire, "Endovascular skills training and assessment," *J. Vasc. Surg.*, vol. 46, no. 5, pp. 1055–1064, 2007.

[99] E. Mazomenos, P.-L. Chang, R. Rippel, A. Rolls, D. Hawkes, C. Bicknell, A. Desjardins, C. Riga, and D. Stoyanov, "A survey on the current status and future challenges towards objective skills assessment in endovascular surgery," in *2016 International Conference on Information Processing in Computer Assissted Interventions*, 2016 (in press).

[100] G. Smoljkic, D. Reynaerts, J. Vander Sloten, and E. Vander Poorten, "Compliance computation for continuum types of robots," in *Intelligent Robots and Systems (IROS 2014), 2014 IEEE/RSJ International Conference on*, Sept 2014, pp. 1066–1073.

[101] E. Aertbelien and J. De Schutter, "etasl/etc: A constraint-based task specification language and robot controller using expression graphs," in *Intelligent Robots and Systems (IROS 2014), 2014 IEEE/RSJ Int. Conf. on*, Sept 2014, pp. 1540–1546.

[102] G. Smoljkic, G. Borghesan, D. Reynaerts, J. De Schutter, J. Vander Sloten, and E. Vander Poorten, "Constraint-based interaction control of robots featuring large compliance and deformation," *Robotics, IEEE Transactions on*, vol. 31, no. 5, pp. 1252–1260, Oct 2015.

[103] M. Edgington, Y. Kassahun, and F. Kirchner, "Using joint probability densities for simultaneous learning of forward and inverse models," in *IEEE IROS International Workshop on Evolutionary and Reinforcement Learning for Autonomous Robot Systems*, N. T. Siebel and J. Pauli, Eds. o.A., 10 2009, pp. 19–22.

[104] B. Yu, A. Tibebu, J.-H. Metzen, and Vander Poorten, "Towards catheter trackign and data-based catheter steering," in *Proc. 5th Joint Workshop on New Technologies for Computer - Robot Assisted Surgery*, 2015, pp. 155–157.